Department of Precision and Microsystems Engineering

Avoiding excessive zero crossings in reset control

Shrinath Diwakar

Report no	:	MSD-2021.064
Coach	:	Nima Karbasizadeh
Professor	:	Dr. S.H. HosseinNia
Specialisation	:	Mechatronic System Design
Type of report	:	MSc Thesis
Date	:	26th August 2021

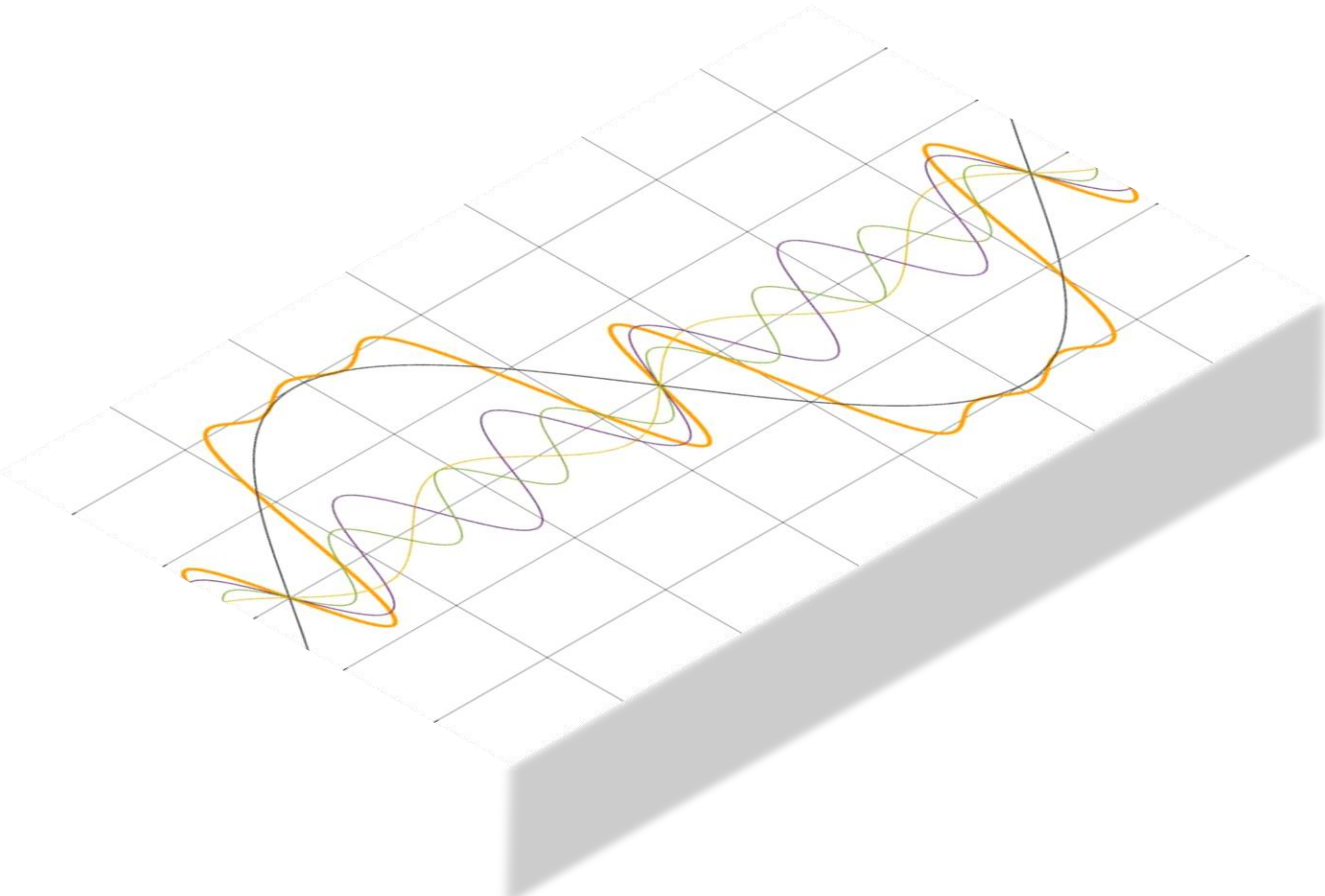

TU Delft Delft University of Technology

Challenge the future

Avoiding excessive zero crossings in reset control

by

Shrinath Diwakar

For the degree of Master of Science in Mechanical Engineering at Delft University of Technology
To be publicly defended on 26 August 2021 at 9:00 AM

Student number:	5011469
Supervisor:	Dr. S.H. HosseinNia Nima Karbasizadeh
Thesis committee:	Dr. D. Boskos Dr. S.H. HosseinNia Nima Karbasizadeh

Abstract

In the present world, a new development in technology every other year is anticipated. Robots and motion stages in the high-tech sector are required to work at higher speeds being stable, more precise, and power-efficient. Linear controllers have served well but are falling short to continue with the trend. Reset elements can enhance the performance of linear filters like PID by overcoming the bounds of linear control. As the name implies, reset elements reset their state/ states, thus induce nonlinearity. This nonlinearity provides reduced phase lag with similar magnitude behaviour as linear elements. With such behaviour or by adding linear filters with reset elements, both the steady-state and transient response can be improved. The tracking precision is not needed to be compromised over stability and noise rejection.

The reset control has its downsides. The resetting action (nonlinearity) produce higher-order harmonics in the output. The number and instant of resets occurring are vital in determining the closed-loop sensitivities. Ideally, only two resets should occur in one period of the reference frequency. But due to higher-order harmonics, multiple resets (zero crossings) can occur, which makes analytical closed-loop estimation difficult. This thesis provides an amplitude threshold criteria on higher-order harmonics to avoid the multiple zero crossings. Controllers following such a threshold can help benefit the system from nonlinearity rather than being adversely affected by it. An example of a control scheme with reset and linear elements for a motion stage is presented that satisfies the amplitude threshold. No multiple resets in the input signal to the reset element for any reference frequency were confirmed.

A novel method to avoid excessive zero crossings is proposed. This method puts a cap on the magnitude of higher-order harmonics. A stepwise procedure is presented to calculate such a threshold.

Acknowledgement

I would like to thank my supervisors Nima Karbasizadeh and Hassan HosseinNia for providing me with an opportunity to pursue my thesis in the field of reset control and become a part of the Mechatronic System Design (MSD) group. Both the supervisor have provided me with great support throughout the journey. Our weekly meetings helped me sustain the curiosity of trying a new direction and learning something new. I was always amazed by the fact that at the end of our long meetings we would come with a promising direction for a problem I was stuck at.

I appreciate the Monday Meetings held by Hassan HosseinNia and Jo Spronck in the MSD group. These meetings provided a perfect kick-start to the motivation after a weekend. This meeting is an amazing platform to learn about the work of other members and discuss problems. Every Monday I used to find something new, outside my knowledge which inspired me. Thank you Hassan and Jo for some of the valuable advice.

I would also like to thank Niranjan Saikumar for helping me with Matlab simulations. Ali Ahmadi Dastjerdi thank you for the introductory video on the spider setup (MSD lab) and for supporting me with Labview files.

I would like to thank TU Delft for giving me a chance to pursue my masters in mechanical engineering. Thank you for providing amazing courses with great facilities. These two years have changed my perspective towards other disciplines and made me more curious to learn more about them. Thank you all my HTE friends for helping me with the coursework and thesis.

Thank you to all my friends and family in India for their endless support. I cannot thank enough my parents for everything and for guiding me to become the person I am today.

Contents

1 Introduction

1.1 Motivation

Semiconductor chips have become an integral part of our lives. From the simplest of the gadgets to the most complicated, all use some form of electronic hardware. For instance, the kettle in the kitchen to elevators to smartphones and computers. To govern the operations of such a gadget, control systems come into the picture. A control system consists of a plant (gadget/ device), sensors, actuators (motor/ piezo) and a controller. To give an analogy to the human body, the controller is the brain, sensors are the sensory organs, actuators are muscles/organs and the plant is any activity being carried out by the body. Some examples where a controller plays a vital role: controlling the position of valves in the pipelines to main a certain pressure, controlling the operation of a compressor in refrigerators and air conditioners to maintain a certain temperature, controlling the orientation and position of satellites, etc. This report focuses on the application of control theory for precision motion in mechatronic systems.

Precision motion is very important when it comes to building machines that produce chips. As the chips are geometrically small with respect to human scale, these chip manufacturing machines have a micrometer to nanometer accuracy. To given a reference, the thickness of a regular $A4$ paper is 0.1 mm. These chip manufacturing machines have to position themselves with an accuracy that is 3 to 6 order less than the thickness of a paper with high speeds. As of now, there is a major shortage of semiconductor chips. Due to this shortage, many industries have to halt their production. The demand for precise and faster machines in the high-tech sector is high. The Fig. 1, [1] shows an extreme ultraviolet lithography (EUV) machine produced by ASML (Netherlands), which is the most advanced chip-making lithography technology to date. These machines are capable of producing chips on 3 and 5 nanometer node. In the Fig. 1, there is a wafer motion stage at center-bottom. This wafer motion stage needs to have an accuracy of sub-micrometer and less with a high frequency of operation. These wafers are feed to the motion stage by a wafer handler produced by VDL. These wafer handlers need to grip the wafer with micrometer accuracy and transport them at high speed. The Fig. 2a, [2] shows the dicing of a silicon wafer to separate chips. These robots are used by chipmakers like TSMC, Nexperia, Intel, Samsung, etc. Such a robot needs to operate in micrometer range with settling time in milliseconds. After dicing, chips are extracted or picked as shown in Fig. 2b, [3]. These extracting chips, need to be soldered on base with high repeatability and accuracy. All examples above demonstrate the significance of precision motion in the semiconductor industry.

To achieve precise motion, the machines are designed and manufactured with strict tolerances. But the system also has errors from disturbance and noise which cannot be accounted for in the mechanical design part. To achieve the desired motion with a cap on error, linear control has been used by the industry for more than a half-century. Linear control systems can be analysed in the time and frequency domain. The time-domain analysis shows how the system responds as time progresses but does provide any information on modes which is very vital for mechatronic systems. The frequency-domain analysis provides information on modes, control input and noise and disturbance rejection. PID controllers have been the backbone of the high-tech industry as they can be analysed in the frequency domain and have good implementability. PID filters can be visualised as a virtual mass spring damper system added to the plant to correct for error and follow a reference. PID being linear, superposition principle is valid. Therefore it is easy to predict error with multiple inputs to the system. The linear control theory comes with the disadvantage of the Bode gain-phase relation and waterbed effect. These limitations restrict linear control systems to achieve the desired system requirements.

To overcome the limitation of linear control, nonlinear control is looked upon. Nonlinear systems are usually analysed in the time domain as they produce higher-order harmonics of a reference. Hence, it is difficult to approximate the system in the frequency domain. But time-domain analysis is not very useful for precision systems as discussed earlier. Reset control is a branch of nonlinear control where the integrator filter in PID is reset to a certain value when a certain condition is

Figure 1: EUV machine by ASML

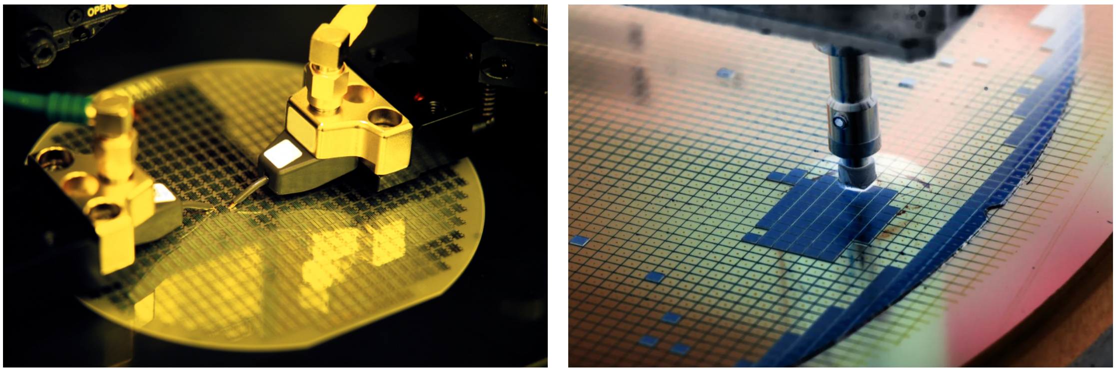

(a) Silicon wafer dicing

(b) Pick and place machine for chips

Figure 2: Precision motion in semiconductor industry

met. Usually, this condition is zero crossings of the input signal to reset element. In other words, some nonlinearity is induced in the linear integrator filter to overcome the limitations of linear control theory. The main advantage of reset control is that it can be well approximated in the frequency domain using higher order sinusoidal describing function analysis. Thus, we can benefit from frequency domain analysis while overcoming linear control theory limitations. As frequency domain analysis (loop-shaping) is widely used by industry, implementation of reset elements is an add-on to the existing filters.

The reset integrator known as Clegg's integrator was introduced by JC Clegg [4] in 1958. This integrator resets its output to zero when the input to it crosses the zero line. The integrator is not allowed to complete its entire cycle, which creates less phase lag. At high frequencies, the phase of linear tends to $-90°$, while the reset integrator tends to $-38°$. Later, using reset integrator, First Order Reset Element (FORE) [6] was introduced. FORE is the reset version of the first order low pass filter. Further, adding a lead in series with FORE makes a Constant in Gain Lead in Phase (CGLP) filter. A CGLP is a lead element, an add-on to the derivative filter in PID. Resets elements can be used as phase compensators. Recently, more reset elements like SORE [5], SOSRE [8] and

FOSRE [7] were introduced. All of the above reset elements are discussed in the next chapter.

Reset control overcomes the Bode gain-phase relation and waterbed effect. But also comes with some downsides. As the integrator resets, there is a sudden jump in the state of an integrator. This jump makes the system nonlinear and hence produces higher-order harmonics in the output. These higher-order harmonics can excite the other modes in multimodal systems, which is undesired. Predicting closed-loop performance from an open loop is difficult as the higher-order harmonics are fed back to the controller and creating a multi-sine input. As the reset element reset when the input to the controller crosses zero, a multi-sine can have more zero crossings than the reference frequency due to higher-order harmonics. This will make the reset element reset more times, more jumps and hence more nonlinearity. Having multiple zero crossings in one period of input makes the closed-loop estimation by the analytical method difficult. In this thesis, a method is proposed which provides a threshold on how low (magnitude) the higher-order harmonics should be to avoiding excessive zero crossings.

1.2 Report Outline

This report consists of five chapters. Chapter 2 provides an overview of the state of the art of reset control in a paper format. It covers the fundamentals and some recent developments. Chapter 2 discusses the problem statement of this thesis. It consists of one main question along with a few sub-questions that need to be tackled. Chapter 4 is the main part of this report presented in a paper format. It proposes a solution to the questions in chapter three. Chapter 5 provides a conclusion along with recommendations. The report also consists of seven appendices. Appendix A presents an alternative amplitude distribution that can be used for any reset system that attenuates with -2 slope. Appendix B consists of an additional example to validate the theory in chapter 4. Appendix C and D provides more insight on chapter 4. Appendix E and F present system identification and stability analysis of reset system respectively. Appendix G provides MATLAB code for the simulations in the report.

2 Literature review

This chapter presents a literature study (review) on reset control systems in a paper format. The literature review initiates with a general introduction to linear and resets control. Section II captures the limitation of linear control. Next, section III review the basics of reset control, its state-space formulation and the higher-order sinusoidal describing functions analysis for frequency response approximation. Section IV covers the state of the art reset elements with their frequency domain response. Section V provides a summary of a recently developed method on band-passing the nonlinearity (higher-order harmonics) of a reset element. Using such a method, the higher-order harmonics can be restricted to a certain band such that the system behaves close to linear outside the band. Section VI presents two methods to compute the closed-loop response of the reset control system. Section VII discusses the effect of different sequences of linear filters and reset element on closed-loop performance, noise rejection, etc. Section VIII illustrates the effect of multiple zero crossings (resets) in reset signal on the closed-loop performance, guiding to the problem statement of this thesis. Section IX as thesis objective and conclusion.

Literature study of reset control systems

Shrinath Diwakar, Nima Karbasizadeh, S. Hassan HosseinNia

***Abstract*—This literature study reviews the recent developments in the field of Reset Control (RC) theory. Reset control overcomes the drawbacks of linear control like Bode gain phase relation and Waterbed. Reset elements like CGLP, FOSRE, etc can provide a phase lead with constant magnitude behaviour. The main drawback of RC is the generation of higher-order harmonics. Recently, a new structure for single state reset elements was proposed which restricts the higher-order harmonics to a band. Due to these harmonics, the close loop analysis becomes complex as. There are two methods proposed to analyse the closed-loop behaviour of RC using the open-loop, first is by using a virtual harmonic separator and second by describing the reset element using state-dependent impulses. Again, in the closed-loop the order of linear and reset filters have a different impact on tracking and noise rejection. The quirks and hitches of the state of the art in RC are presented in this paper.Last, the problem statement for this thesis is presented.**

***Index Terms*—Nonlinear control, Reset Control (RC), reset elements, higher-order harmonics, describing function, motion control**

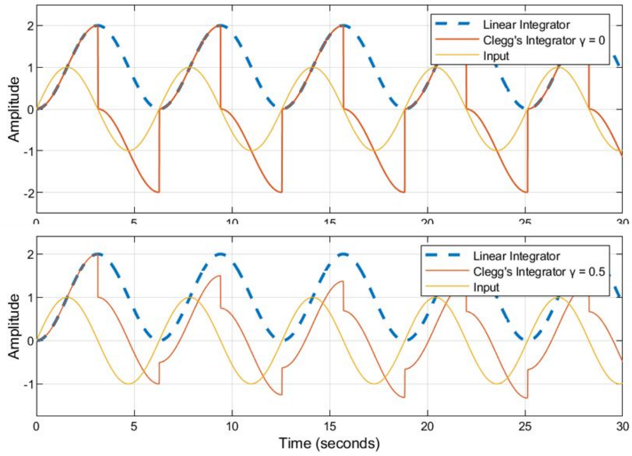

Fig. 1: Simulation of Clegg's Integrator

I. Introduction

The world is moving towards miniaturization every day. Electronic circuits are getting smaller and more power-efficient. The smartphone processors are developed on a scale of 5 nm till date. The sensors used in automobiles, heavy machinery, etc are moving towards nano-meter scale. To sustain this progress, we need machines that are cable of moving and sensing small movements. For doing so control systems play an important role, especially PID controllers. PID controllers have been used in the industry for about a century. PIDs cover the majority share of the various controllers available to the industry. The reason behind this is the ease of implementability and tunability. The analysis of PIDs in the frequency domain paves the way to capture more information of the modes and system behaviour at a wide range of frequencies.

Linear controllers come with limitation like Bode gain phase relation. Ideally, high bandwidth is desired and a phase lead around bandwidth to assure system stability. Improving the tracking performance can be done by adding integrator. Doing so results in phase reduction at the bandwidth. As a result, system tracking and robustness contradict each other. In other words, if one improves other degrades. Another limitation of PID is the Waterbed effect [1], where the betterment of noise reduction at a certain frequency will worsen the same at other frequency. There are other limitations like integral windup and saturation as well. Due to all these limitations, PID cannot be used to achieve all the system requirements.

To overcome the limitations mentioned above Nonlinear controllers are brought in the perspective. Reset control is a branch of nonlinear controllers which is becoming popular as of now. A rest controller resets its state/ states to a certain value when a certain condition is met. Doing so creates a phase advantage of keeping the same gain characteristics. Nonlinear systems are generally analysed in the time domain which makes the implementation difficult in practice. Describing function analysis is used to transform the time domain study into frequency domain approximation, which eases the implementation with loop shaping method.

In the late 1950s, JC Clegg introduced the first reset element as Clegg's Integrator (CI) [2]. The time-domain response of a linear integrator (LI) and CI is compared in Fig. 1. The CI resets its output when the input signal crosses the x-axis. The reset value in Fig. 1 (upper sub-figure) is set to zero but it can vary anywhere between its positive and negative amplitude span. This resetting action provides a phase advantage of 52 degrees over the LI. The gain of CI has the same slope as of LI but slightly high gain. This idea of CI was further used to develop many other resets elements namely First Order Reset Element (FORE) [3], Second Order Reset Element (SORE) [4], Constant Gain Lead Phase (CGLP) [5], Fractional Order Single State Reset element (FOSRE) [6], etc. These elements have similar magnitude characteristics but different phase behaviour as compared to linear lead and bandpass pass filters.

Reset controllers (RC) are broadly used as wide-band phase compensators. As discussed earlier, RC provides phase lead with zero gain behaviour and thus increase the phase margin available at the bandwidth. The rise time and overshoot performance are improved as well. Many engineering domains have utilised RC for improving the performance, thermal [7], chemical [8], vibration control [9], precision motion control [5]. The reset controllers have a downside as well. It can be seen from the Fig. 1, at reset instants there is a sudden jump in the state of the controller. This introduces a high degree of nonlinearity into the system and thus higher-order harmonics in the output. These high order harmonics can adversely affect the system if they are not considered along with the describing function approximation. Also, RC can introduce limit cycles in the output if the steady-state error is not zero. To counter the limit cycles many strategies has been developed like partial reset, $CI + PI$ control [10] , adding feed-forward [11] [12].

The structural outline of this paper is as follows; section II briefly discusses the limitation of PID. Section III captures preliminaries of reset control. Section IV gives an overview of the reset elements. Section V discuss the band passing the non-linearities. Section VI explains the stability of nonlinear controllers. Section VII encapsulate the open-loop to close loop behaviour for reset control. Section VIII presents an optimal order for linear and reset elements in the closed-loop. Section IX provides the problem statement for the thesis followed by the conclusion.

II. Limitation of PID

The Proportional Integral Derivative control (PID) is widely used in industries for all types of control systems. In motion control, PID is analogous to a virtual mass spring damper system. The role of a control system is to make system stable (robust), track the input signal, reject disturbance and noise. These requirements can be translated in the frequency domain as the phase advantage around bandwidth, high gain at low frequencies and low gain at high frequencies, respectively. PID being linear has its benefits of superposition, commutation, etc. Having these benefits comes at a cost of being bounded by some conditions such as bode gain phase relation, waterbed effect, etc.

A. Bode gain phase relation

In a Bode plot of any linear filter, the slope of the magnitude plot has a certain phase associated with it. For instance, for an integrator, the slope of the magnitude plot will be -1 and the phase will be $-90°$. If there is a double integrator, the slope will be -2 and the phase will be $-180°$. The Eq. 1 represents the relation between the slope of magnitude and phase. So, to have phase lead around bandwidth, the magnitude slope has to positive. It is not possible to circumvent this relation staying in the linear domain.

$$\angle G(j\omega) = 90° n \tag{1}$$

where, G is a linear filter and n is the slope

B. Closed loop Sensitivity functions

The Fig. 2 shows a block diagram of a generic closed-loop system with $C(s)$ and $G(s)$ as the controller and plant respectively, $r(t)$ and $n(t)$ as the reference and noise respectively, $y(t)$ as the output. In precision motion control, for an open-loop $CG(s)$ bode plot it is desired to have a very high gain at low frequencies and a very low gain at high frequencies.

There are four closed-loop sensitives, out of which the Eq. 2 represents two as the Sensitivity function $S(s)$ and Complementary Sensitivity function $T(s)$. The first is influenced by the noise and the second by reference. At low frequencies, the $T(s)$ will have a high magnitude then $S(s)$ to have better tracking but poor noise rejection. The condition but reversed at high frequency. To have a stable system, a sufficient phase margin is needed around the bandwidth. For achieving this phase lead, the slope of the magnitude has to be increased which in turn increases the $T(s)$ which is undesired at high frequency. The robustness is achieved at the cost of amplification of noise. The two sensitivity functions related by Eq. 3 for all frequencies. There is always a trade-off between noise rejection and tracking. In linear PID having robustness, tracking and good noise rejection at a certain frequency are not possible.

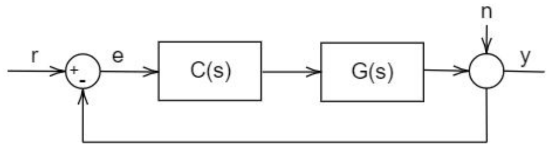

Fig. 2: Closed loop system

$$S = \frac{y}{n} = \frac{1}{1+CG} \quad , \quad T = \frac{y}{r} = \frac{CG}{1+CG} \tag{2}$$

$$T(s) + S(s) = 1 \tag{3}$$

C. Waterbed effect

The Eq. 4 represents the Sensitivity function $S(s)$ for any frequency. The integral represents the area of $S(s)$ below and above 0 dB line. If the magnitude of $S(s)$ is reduced at one frequency then it will be increased at some other frequency to nullify the area below and above 0 dB line to satisfy the Eq. 4. This effect is known as the waterbed effect in control theory. We can not have good noise rejection at all frequencies.

$$\int_0^\infty \ln|S(j\omega)| d\omega = 0 \tag{4}$$

III. Preliminaries of Reset Control

A. State space formulation

The Eq. 5 represents a generalised state space formulation of a reset controller (RC) [13]. A, B, C, D are state matrices of the RC. A_ρ represents the reset matrix. When the input $e(t) = 0$, the current states $x(t)$ gets resets to certain value according to A_ρ. If $e(t) \neq 0$, the state space follows the base linear form for the RC.

$$\sum\nolimits_R = \begin{cases} \dot{x}_r(t) = Ax_r(t) + Be(t) & \text{if } e(t) \neq 0, \\ x_r(t^+) = A_\rho x_r(t) & \text{if } e(t) = 0, \\ u(t) = Cx_r(t) + De(t) \end{cases} \tag{5}$$

In the above case, the reset condition is set to zero crossings of input $e(t)$ but that can be altered. The zero-crossing law is linear in gain (amplitude) and nonlinear in frequency. Other reset laws like reset band can be found in [14] [7] where, if the input $e(t)$ is in the band zone the reset occurs. Extending the reset band, the states can be reset only when the input $e(t)$ enters or leaves the reset band. Reset bands can help combat the delay but do introduce nonlinearity with gain. For MIMO systems, different reset laws can be implemented for different inputs but increase the complexity.

B. Nonlinear System Analysis in Frequency Domain

On a general scale, the nonlinear systems are analysed in the time domain which is very well suited for certain applications like population dynamics, flow dynamics, etc. But in control theory, the time domain does not provide enough information about the system. Hence, the study is switched to the frequency domain. For nonlinear systems, switching to frequency domain is complex due to nonlinear effects like inter-modulation, desensitization, harmonics and input dependent gain [15]. To switch in the frequency domain, many paths can be found in literature such as describing function (DF), higher-order sinusoidal describing function (HOSIDF), Volterra series, linear approximations for nonlinearity, etc. In [15], a comparative study of such methods for nonlinear effects is done. Not all methods can capture all the nonlinear effects. along with the information about the gain and phase of input and output.

C. Describing Function (DF)

Consider nonlinear systems as a block with time-dependent input and output. The transfer functions of this block are not known. From the steady-state output signal in the time domain, using the Fourier Series approximation, the output signal is converted into the frequency domain using only the first fundamental frequency of the series known as Describing function. DF has been extensively used to study nonlinear control systems since the second half of the 20^{th} century. In motion systems, periodic inputs are very common. If the input is sinusoidal, the DF becomes Sinusoidal Input DF (SIDF). Guo et al. in [16] and [17], presented a SIDF (no phase difference in input) analysis for reset systems with input $e(t) = 0$ as the reset instants. The equation 6 provides a frequency-domain approximation of a reset system A, B, C, D as its state matrices. SIDF analysis provides the gain and phase information of input frequency as only the fundamental frequency of Fourier is used for the approximation. The Fig. 3 shows the SIDF frequency response (only the 1st Harmonic) of Clegg's integrator.

$$G(\omega) = C(j\omega I - A)^{-1}(I + j\Theta(\omega))B + D \tag{6}$$

where,

$$\begin{aligned}
\Theta_D(\omega) &= \frac{-2\omega^2}{\pi}\triangle(\omega)[\Gamma_r(\omega) - \Lambda^{-1}(\omega)] \\
\Lambda(\omega) &= \omega^2 I + A^2 \\
\triangle(\omega) &= I + e^{\frac{\pi}{\omega}A} \\
\triangle_r(\omega) &= I + A_\rho e^{\frac{\pi}{\omega}A} \\
\Gamma_r(\omega) &= \triangle_r^{-1}(\omega)A_\rho\triangle(\omega)\Lambda^{-1}(\omega)
\end{aligned} \tag{7}$$

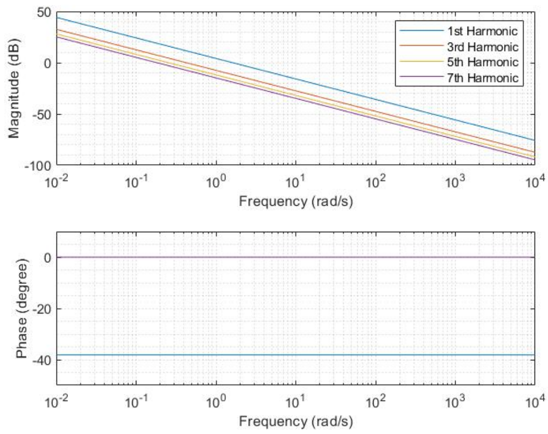

Fig. 3: Clegg's integrator with higher harmonics

D. Higher Order Sinusoidal Input Describing Function (HOSIDF)

For nonlinear systems, it is known that for an input of certain frequency, the output will higher-order harmonics of input frequency along with different gains for each [18]. The SIDF only encapsulates the input gain dependent nonlinear effect and not the others. Along with this, DF analysis does not provide any gain-phase information of frequencies not present in the input. Therefore, SIDF analysis is not accurate enough to approximate a reset system. Heinen et al. in his thesis [19], extended the DF analysis in [17] and presented HOSIDF. HOSIDF approximates the reset system using Fourier series with higher frequencies included. The Eq. 8 presents the HOSIDF expression for reset systems. The input and output being an odd function, the higher even harmonics are zero and only odd harmonics exist. Each harmonic will have its transfer function, where n in Eq. 8 represents the harmonic number.

$$G_n(\omega) = \begin{cases} C(j\omega I - A)^{-1}(I + j\Theta(\omega))B + D & n = 1 \\ C(j\omega nI - A)^{-1}j\Theta(\omega)B & n_{odd} > 2 \\ 0 & n_{even} \geq 2 \end{cases} \tag{8}$$

In Fig. 3, the higher harmonics of Clegg's integrator are shown. The higher-order harmonics have less magnitude and zero phase contribution compared to first harmonic. Not considering the higher harmonics while designing a reset system can be erroneous and can cause the nonlinearity as a disadvantage. Such an example is provided later in the Reset Elements section (CGLP) of the paper.

E. Stability of reset control systems

In linear systems, the BIBO stability can be checked from Nyquist plot or Bode plot. In the case of nonlinear systems, checking phase or gain at certain points does not ensure stability. In [19], some cases are presented for reset systems where all the phase and gain criteria are not fulfilled and the system still is BIBO stable. The principle of dissipation of energy with time is to be followed.

For reset systems, first the base linear system should be BIBO stable. To inspect the quadratic stability H_β condition should be fulfilled [20] [13].

Theorem 1. *There exist a $\beta \in \Re^{n_r \times 1}$ and positive definite matrix $P_\rho \in \Re^{n_r \times n_r}$, such that the restricted Lyapunov equation*

$$P > 0,\ A_{cl}^T P + P A_{cl} < 0 \tag{9}$$

$$B_0^T P = C_0 \tag{10}$$

has a solution for P, where

$$C_0 = \begin{bmatrix}\beta C_p & 0_{n_r \times n_{nr}} & P_\rho\end{bmatrix}, B_0 = \begin{bmatrix}0_{n_p \times n_r} \\ 0_{n_{nr} \times n_r} I_{nr}\end{bmatrix} \tag{11}$$

and,

$$A_\rho P_\rho A_\rho - P_\rho \leq 0 \tag{12}$$

A_p, B_p, C_p, D_p are state matrices of the plant, A_{cl} is the closed-loop (controller and plant) state A matrix. n_r are the number of states being reset, n_{nr} are states not being reset and n_p are the number of states of a plant.

IV. Reset Elements

A. FORE and SORE

Taking the Clegg's integrator ahead, Horowitz et al. in [3] introduced First Order Reset element (FORE). FORE is reset version of linear first-order low pass filter (LPF). The Eq. 13 shows the analytical expression of FORE with w_r as the corner frequency. In the Fig.4 the frequency response (FRF) of FORE is shown with a corner frequency of 10 rad/s along with higher-order harmonics. If only the first harmonic is considered, then the response of FORE is similar to that of LPF at low frequencies, though at frequencies we can see the added phase by the resetting action maintaining the Magnitude behaviour. The first harmonic phase at high frequency tends to $-38°$ and not $-90°$. Coming to the higher-order harmonics, they are most dominant around corner frequency.

Generalised FORE (GFORE) [17] was introduced further ahead. In Fig. 4 the FORE has only w_r as the variable and $A_\rho(reset\ value = 0)$ is constant. GFORE has two variables in w_r, $A_\rho = \gamma$, where $\gamma \in (-1, 1)$. Varying the γ affects the phase advantage and dominance of higher order harmonics. For $\gamma = 1$, the filter has no non-linearity has behaves like a linear LPF. Such affects of γ can be seen in following section SORE.

$$FORE = \frac{1}{\cancelto{A_\rho}{\frac{s}{\omega_r}+1}} \quad SORE = \frac{1}{\cancelto{A_\rho}{(\frac{s}{\omega_r})^2 + \frac{2s\beta}{\omega_r} + 1}} \tag{13}$$

Second-Order Reset Element (SORE) was introduced by Hazelgar et al in [4]. SORE is the reset version of Second-order low pass filter (SLPF). The Eq. 13 shows the expression of SORE with w_r and β as variables. The parameter β also makes it possible to have a notch and anti-notch like behaviours. The Fig. 5 shows the FRF plot for the first harmonic. The higher-order harmonics have a similar response

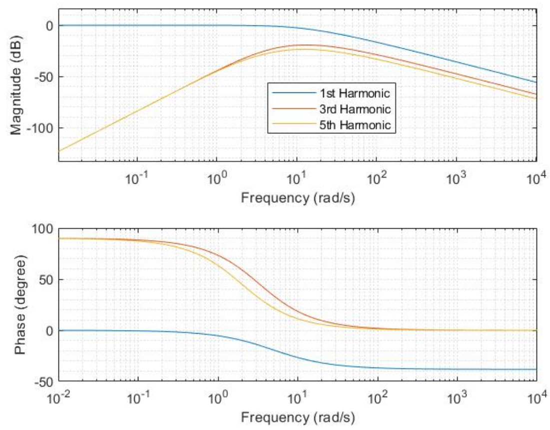

Fig. 4: First order reset element

as that in FORE. As it can be seen that the phase tends to $-52°$ and not $-180°$ as in SLPF.

Similar to GFORE, Hazelgar et al in [4] extended SORE to Generalised SORE (GSORE). GSORE adds one more variable $A_\rho = \gamma I_{2\times2}$, where $\gamma \in (-1, 1)$. Again the effect of γ on higher-order harmonics is similar to that of GFORE. The Fig. 5 shows the first harmonic behaviour for various γ. As γ tend to 1, the phase advantage diminishes and the GFORE is SLPF.

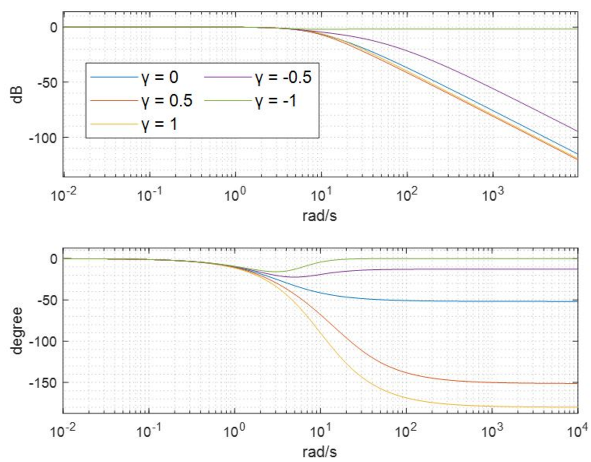

Fig. 5: Second order reset element

B. CGLP

Constant in Gain Lead in Phase (CGLP) is a reset element recently developed by Saikumar et al. [5]. GGLP provides phase lead over a range of frequencies with a constant gain behaviour. This element is an alternative to the lead filter in PID. Using GFORE or GSORE in series with corresponding order lead filter forms a CGLP. The Eq. 14 is a second-order CGLP with w_r and w_f as the range in which phase lead is obtained. Due to resetting action, a shift in the corner frequency is observed. To compensate this change a variable α is introduced such as $w_r = \alpha\, w_{r\alpha}$. The phase lead is provided by the first harmonic. The Fig. 6 shows the FRF of $1^s t$ order

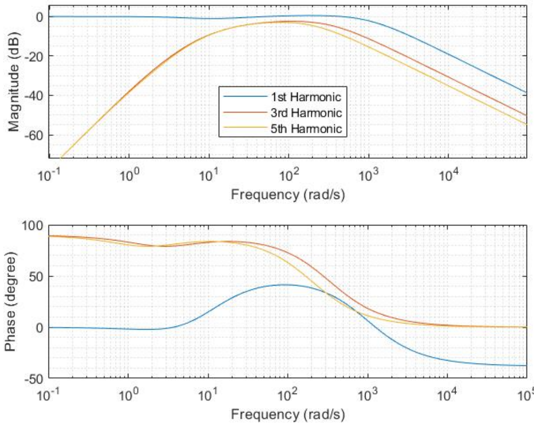

Fig. 6: CGLP 1^{st} order

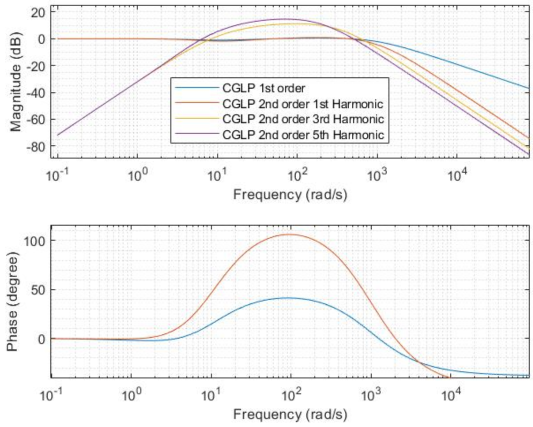

Fig. 7: CGLP 2^{nd} order

CGLP along with higher-order harmonics with $w_r = 10rad/s$ and $w_f = 1000$ rad/s. A phase lead of $42°$ is obtained at 100 rad/s with $\gamma = 0$.

A_ρ

$$\begin{aligned} R(s) &= \frac{1}{(s/\omega_{r\alpha})^2 + 2s\beta/\omega_{r\alpha} + 1} \\ D(s) &= \frac{(s/\omega_r)^2 + 2s\beta/\omega_r + 1}{(s/\omega_f)^2 + 2s/\omega_f + 1} \\ CGLP &= R(s)\, D(s) \end{aligned} \tag{14}$$

A comparison between 1^{st} order and 2^{nd} order CGLP is shown in Fig. 7. From the phase plot, it can be seen that phase advantage provided by the second-order CGLP is around $108°$ with almost constant gain characteristic. A linear controller cannot achieve this due to Bode Gain Phase relation, the slope of magnitude has to increase to provide phase lead. From the Eq. 14 it can be seen that there is a variable β which accounts of damping performance of the filter. In the magnitude plot of Fig. 7, the 3^{rd} and rest of the higher harmonics are more dominant than the 1^{st} harmonic due to values assigned to variables (here $\beta = 1$). Hence the DF analysis is not accurate enough and HOSIDF analysis is needed.

As discussed in the stability of reset elements section, a linear PID should be designed which makes the close-loop system stable and only then the reset elements can be added. Salman et al. in [21] tuned the 1^{st} order CGLP using parameters γ and $\omega_r = f(\omega_c)$ for a certain phase margin to have the minimum RMS tracking error, where ω_c is the bandwidth frequency of the linear controller. Hou et al. in [22] tuned both the 1^{st} and 2^{nd} order CGLP using the various γ and ω_r to obtain different phase lead at ω_c to minimise noise and RMS tracking error. Different combination of γ and ω_r can lead to same phase margin but have different higher-order harmonics. Lesser the magnitude of higher-order harmonics better is performance.

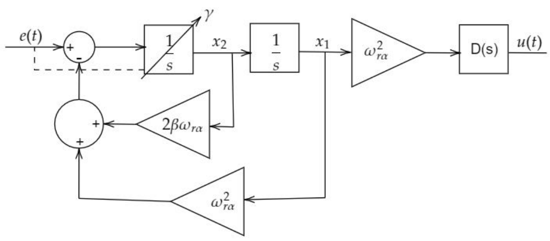

Fig. 8: SOSRE block diagram

C. SOSRE

Taking the 2^{nd} order CGLP further ahead, Nima et al. introduced Second-Order Single state Reset Element (SOSRE) in [23]. In the 2^{nd} order CGLP, both the states are reset to $A_\rho = \gamma$. The expression of SOSRE is same as in the Eq. 14. The Fig. 8 represents the block diagram of SOSRE, in which only one state is being reset. Resetting this specific state only results in a notch like behaviour at $w_{r\alpha}$. Fig. 9 is the FRF of SOSRE. The first harmonic behaviour is the same as the CGLP but a notch is present at a particular frequency ($w_{r\alpha} = 6.5$) rad/s for higher-order harmonics. At this $w_{r\alpha}$ frequency, we have no phase advantage but all the higher-order harmonics are very small comapred to first harmonic. If one operates at this $w_{r\alpha}$ as the reference, the filter will behave like a linear lead filter.

Let ψ be the phase difference between the input and output resetting state as shown in Eq. 15. The reason behind the notch like behaviour is the that at this frequency the phase difference $\psi = 0$. Therefore when the input is zero, the output should reset to γ but the out is already at zero being $\psi = 0$. Hence the resetting does not affect output and the SOSRE behaves like a linear filter. The frequency response of ψ is shown in Fig. 10, around $w_{r\alpha} = 6.5$ rad/s the zero phase difference can be seen.

$$\frac{\angle x_2}{\angle e} = \psi \tag{15}$$

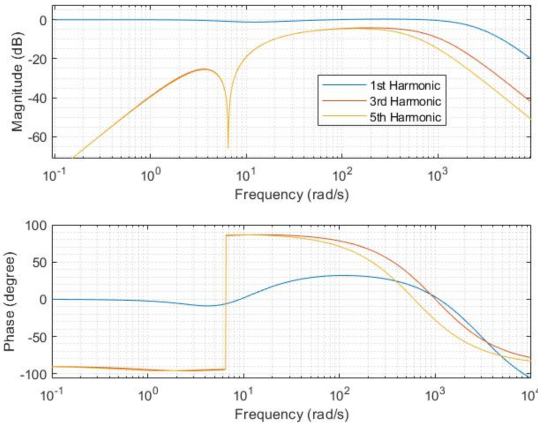

Fig. 9: Second Order Single state Reset Element

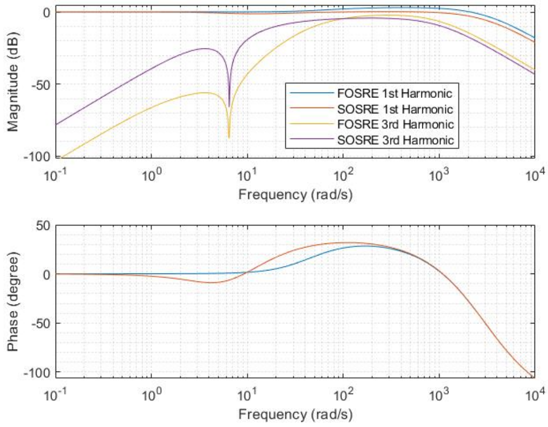

Fig. 11: Fractional Order Single state Reset Element

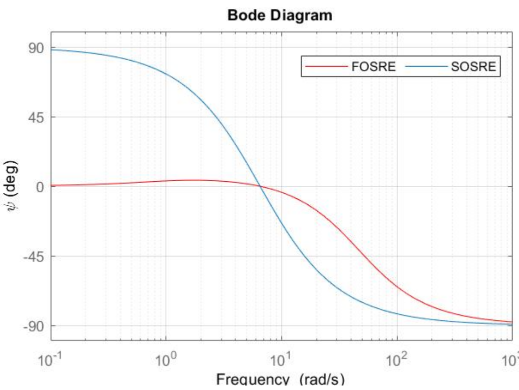

Fig. 10: ψ plot for SOSRE and FOSRE

D. FOSRE

SOSRE provided a way to have a linear behaviour at one frequency, following this trend, Nima et al. developed Fractional Order Single state Reset Element (FOSRE) [6]. The Fig. 10 shows that when $\psi = 0$, we have linear behaviour. FOSRE shapes this ψ to be close if not equal to zero for low frequencies. The Fig. 10 shows the ψ behaviour for FOSRE. The FOSRE intersects SOSRE and $\psi = 0$ line at $w_{r\alpha} = 6.5$ rad/s which produces a notch in FOSRE similar to SOSRE.

The Eq. 16 represents the analytical expression for FOSRE in Laplace domain. The block diagram of FOSRE is similar to Fig. 8 with the second state being a fractional-order state instead of an integer one. A corresponding order lead filter with one sate being of fraction order is in series with FOSRE to form a lead filter. The Fig. 11 shows a comparison between SOSRE and FOSRE. Both the filters are designed to have a notch at $w_{r\alpha} = 6.5$ rad/s, the FOSRE has a lower magnitude in low frequencies than SOSRE for low frequencies with same first harmonic behaviours. This low magnitude is the result of shaping ψ. Since the second state is of fractional order, the reset value γ has to be lower for FOSRE than that of SOSRE for same phase margin, for instance, $\gamma = 0.2$ and 0.4 for FOSRE and SOSRE in figure 11 respectively.

A_ρ

$$FOSRE(s) = \frac{1}{(s/\omega_l+1)^{-\lambda}(s/\omega_{r\alpha}^2 + 2\beta/\omega_{r\alpha}) + 1} \tag{16}$$

$$D(s) = \frac{(s/\omega_l+1)^{-\lambda}(s/\omega_r^2 + 2\beta/\omega_r) + 1}{(s/\omega_f)^2 + 2s/\omega_f + 1}$$

CRONE approximation and Fractional order Calculus:

To calculate the power to a non-integer number we use Taylor's approximation, similarly to calculate the non-integer power of differentiation and integration operation in calculus, Laplace transform is used and then s^λ is approximated where, $\lambda \in \Re^-$. In [24], a toolbox for fractional order control is designed. In this paper the CRONE approximation [25] is used to calculate s^λ, the Eq. 17 represents CRONE. A fractional action is created using N number of poles and zeros lying in left half (stable region) of complex s-plane. In the range from ω_l to ω_h a tamed fractional lead or lag filter can be designed using Eq. 17 and 18. The variable C is used to change the gain of the filter. In this section, a large ω_h is assumed which changes the CRONE approximation to $(s/\omega_l + 1)^\lambda$ and can be directly used in Eq. 16.

$$\left(\frac{s/\omega_l+1}{s/\omega_h+1}\right)^\lambda \approx C\prod_{m=1}^{N}\frac{1+(s/\omega_{z,m})}{1+(s/\omega_{p,m})} \tag{17}$$

where,

$$\begin{aligned} \omega_{z,m} &= \omega_l(\omega_h/\omega_l)^{\frac{2m-1-\lambda}{2N}} \\ \omega_{p,m} &= \omega_l(\omega_h/\omega_l)^{\frac{2m-1+\lambda}{2N}} \end{aligned} \tag{18}$$

V. BAND-PASSING NON-LINEARITY IN RESET ELEMENTS

In the FOSRE, the dominance of higher-order harmonics are kept at a minimum by shaping the phase difference (ψ) between the input and output of reset element to zero. Extending this concept, Nima et al. introduced Band-passing the Nonlinearity in Reset Element (BNRE) [26]. BNRE is only for filters with one state, for instance, GFORE. The Fig. 12 shows the block diagram of Bandpass CGLP reset element.

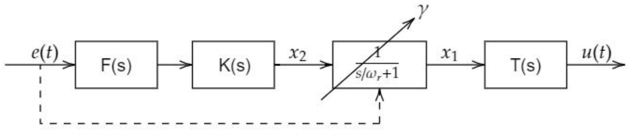

Fig. 12: Block diagram of Bandpass CGLP

As linear filters are placed before the reset element, the DF and HOSIDF equation will change and will result in Eq. 19. If the same filters are placed in the reset line the equations will differ.

$$G_n(\omega) = \begin{cases} f(n,\omega)(1-e^{-j2\psi}) & \\ \quad +C_r(j\omega I - A_r)^{-1}B_r + D_r & n=1 \\ f(n,\omega)(1-e^{-j2\psi}) & n_{odd} > 2 \\ 0 & n_{even} \geq 2 \end{cases} \tag{19}$$

where,

$$f(n,\omega) = C_r(A_r - j\omega nI)^{-1}\frac{\omega e^{-jtan^{-1}(\frac{\omega}{\omega_r})}}{\pi\sqrt{1+(\frac{\omega}{\omega_r})^2}}(1-A_\rho)\delta_\rho^{-1}\delta$$
$$\delta = 1 + e^{\frac{\pi A_r}{\omega}}$$
$$\delta_\rho = 1 + A_\rho e^{\frac{\pi A_r}{\omega}} \tag{20}$$

The Fig. 13, represents the frequency response for bandpass CGLP. The figure is divided into 3 subplots, from top to bottom it represents magnitude, phase and ψ plots. The bandpass CGLP is designed such that the higher-order harmonics are dominant in the range of w_l to w_h (CRONE approximation) and with a bandwidth of 5 rad/s. In the rest of the frequencies, only the first harmonic is dominant. The controller provides a phase of 15° for $\psi = -52°$ and $\gamma = 0.6$. It can be seen that around the bandwidth the higher-order harmonics have most dominant for such the above controller. For a certain bandwidth and phase margin, ψ and γ can be optimised to reduce the dominance of higher-order harmonics.

In the magnitude plot, notches are present just before and after w_l and w_h due the intersection of ψ with the $\psi = 0$ line. For frequency tracking, these notch frequencies are a good choice. Around the bandwidth, the higher-order harmonics have most dominant. The phase lead obtained in the band region is almost constant (flat phase behaviour). This can be used to the advantage of having robustness. This kind of phase behaviour can be modified by changing the shape of ψ, ω_r and range of ψ for accounting a phase lag or any other application. Choosing $w_r < w_l$ will result into the flat phase as observed in Fig. 13, with $w_l < w_r < w_h$, the phase will be of tamed ramp nature. As the linear filters are added before the reset element, the expression for ψ will be Eq. 21 and after a few simplifications as Eq. 23.

$$\psi(\omega) = \frac{\angle x_1}{\angle e} = \angle F(j\omega)\, K(j\omega)\, R(j\omega) \tag{21}$$

where, $R(j\omega)$ is the base linear form of reset element

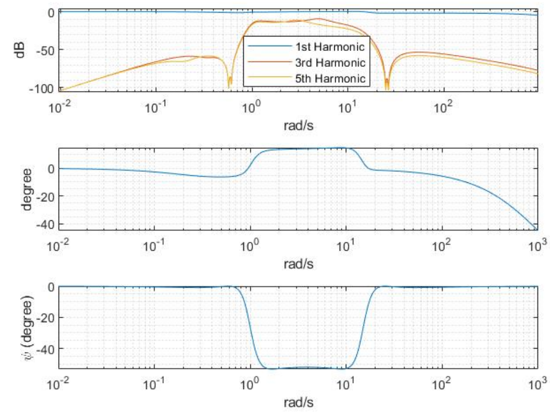

Fig. 13: Bandpass CGLP 1st order

$$K(s) = \frac{s/\omega_r + 1}{s/\omega_f + 1} \tag{22}$$

choosing a high w_f, ψ can be simplified to,

$$\psi(\omega) = F(j\omega) \tag{23}$$

Shaping filter $F(s)$:

The shaping filter $F(s)$ vastly determines the ψ, which in turn is responsible for phase margin and higher-order harmonics. The shaping filter is like a skewed notch filter made from three linear filters, a notch N_2, an anti-notch N_1 and a fractional lag element L_1. The Fig. 14 shows a Bode plot for all three individual filters along with shaping filter. The Eq. 24 represents all the three filters in the Laplace domain. For the fractional lag element L_1, CRONE approximation stated in FOSRE section is used with the same notation and variables. In the notch and the anti-notch filters, there is a damping variable q which can be adjusted to vary the height of the peak. The value of q is chosen in such way that the ψ intersects the 0° line at least once on both the side, that is before ω_l and after ω_h to ensure we notch in higher-order harmonics as discussed before.

$$\begin{aligned} F(s) &= N_1(s)L_1(s)N_2(s) \\ L_1(s) &= \left(\frac{s/\omega_l + 1}{s/\omega_h + 1}\right)^\lambda \\ N_1(s) &= \frac{(s/\omega_l)^2 + s/\omega_l + 1}{(s/\omega_l)^2 + s/(q\omega_l) + 1} \\ N_2(s) &= \frac{(s/\omega_h)^2 + s/(q\omega_h) + 1}{(s/\omega_h)^2 + s/\omega_h + 1} \end{aligned} \tag{24}$$

VI. Open loop to close loop

The controller and plant in series are defined as open loop. If the controller is linear (PID), only one plot is obtained as the output follows the same frequency as input. In reset control, we have multiple harmonics at the output and thus open loop for each. The Fig. 15 shows open-loop plots higher-order

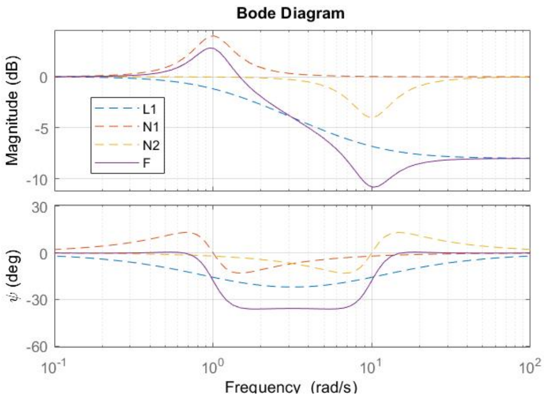

Fig. 14: Shaping filter

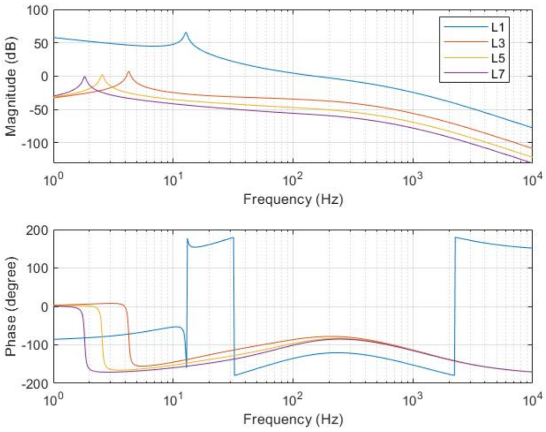

Fig. 15: Open loop (L) with 1^{st} order CGLP

harmonics for a first-order CGLP with a plant (mass-spring damper). The parameters follow the $C04$ controller in [27]. In the Fig. 15 the resonance peaks of higher-order harmonics are visible in low frequency which can have an adverse effect on tracking performance.

In linear control, the closed-loop performance can be estimated accurately with open loop, so is not the case with nonlinear control. If only the first harmonic of the input reference is produced by a controller, in the feedback only that harmonic is fed. If a controller produces multiple higher-order harmonics, then the same will be fed-back to the controller. Now there are multiple sinusoids as an input to controller and each of these sinusoids will produce higher harmonics of their fundamental frequency and the train continues. Now, these multiple frequencies will cause multiple resets. The superposition does not hold for nonlinear systems, it is difficult to predict the output of a closed-loop system when a sum of sinusoids as a reference is provided to the reset controller. These are the biggest drawback of nonlinear control. Reducing the higher-order harmonics or finding a threshold could be a solution.

To estimate the performance of closed-loop reset system (CLRS), numerical and experimental (simulation) methods

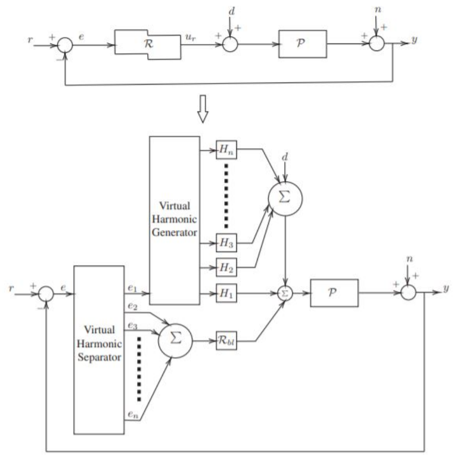

Fig. 16: Block diagram for closed loop system with harmonic separator and harmonic generator [27]

have been applied in the literature. Doing so we get fairly accurate results but does not provide any information about the system dynamics as the analysis is done in the time domain. Recently, Saikumar et al. presented an analytical method to estimate the CLRS from the open-loop [27]. Figure 16 shows a block diagram of CLRS with a harmonic generator and a harmonic separator. The reset system is modelled as a harmonic generator which produces higher harmonics for a fundamental input frequency. These higher harmonics are input to plant and fed back to the controller. To avoid the input of higher-order harmonics of the fundamental frequency to the rest system, a harmonics separator is placed before the harmonic generator which allows only the fundamental first harmonic frequency to input to the harmonic generator. The rest of the harmonics from the feedback are modelled as disturbance input to the plant. There are four assumptions in this method; there are only two resets in one period of fundamental, only the first harmonic of error results in resets and two more. In [27] analytical expressions to estimate the closed-loop sensitivities can be found. In the low-frequency range, this method provides results with an error of less than 1%. But for frequencies close to integrator cutoff and higher, the estimation is not accurate.

Alternatively, Buitenhuis et al. in his thesis [28] proposed a second approach to estimate closed-loop sensitivities from the open-loop. Buitenhuis used state-dependent impulses to estimate the close loop behaviour of reset systems. The reset systems were modelled as base linear systems plus the impulse. These impulses are provided at reset instants and provide an accurate estimation of an open loop system. In [], an elaborate explanation with proofs are presented to calculate these reset instants and hence the closed-loop sensitivities. This method also has assumptions of which one is that only there are only two rests in one period and others. The Fig. 17 shows the block diagram of the reset system with state-dependent impulses and with two linear filters ($G(s)$ and $K(s)$) before and after the reset element. Virtual inputs B^* and Q^* are used to calculate the DF and HOSIDF. This method

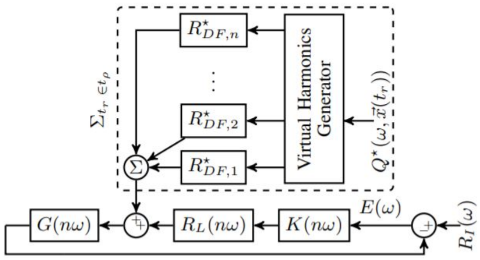

Fig. 17: Block diagram for impulse HOSIDF closed loop system [28]

can also be extended to MIMO systems. The error between the estimation and simulation is well under 1% for low-frequency area. This impulse method provides better results than the harmonic separator method but is more computationally expensive.

VII. Optimal sequence of Filters

We know from the stability of reset systems that we need to have BIBO stability before introducing reset elements. To ensure BIBO we need to have linear PID to stabilize the plant. PI and D are lag and lead filters respectively. In linear systems the order of filters like lead, lag and plant does not matter both in open-loop and closed-loop, any combination will result in the same output as superposition is valid. In the reset systems as superposition does not hold and different order provides different results.

The Fig. 18 shows all the possible sequences of lead, lag, reset with low pass filter (LPF) is shown. In the open-loop, all the sequences provide the same result but in closed-loop different sequence provide a different result. Cai et al. proposed an optimal order for these possible combinations in [29]. From the Fig. 18, sequence 1 and 3 provide the best results for certain criteria and inputs. Sequence 3 is the optimal sequence if there is a low ratio of noise to input amplitude. As the lead filter has a positive magnitude, it amplifies the signal. If the lead filter is placed after the reset elements, the higher-order harmonics will be amplified. As a lag filter has a negative slope in magnitude, it will attenuate the input signal. As the dominance of higher order is to keep at a minimum, the lag filter should be after the reset element in series. The LPF being a lag filter should always be after reset so that the higher harmonics that are input to plant and then to feedback back should be attenuated for best results.

If there is noise in the system, sequence 1 works best as the lag filter just after the reset systems act like a LPF for higher-order harmonics. The same can be achieved with sequence 3 with a LPF in the reset line. Doing so the HOSIDF expression will change as the LPF will introduce a phase lag in the reset instants and so the input has to be altered accordingly. In the [], new HOSIDF is derived for sinusoidal input with a phase lag. This method of introducing a LPF into reset line works only if the noise is less than $2-3\%$ of the reference signal.

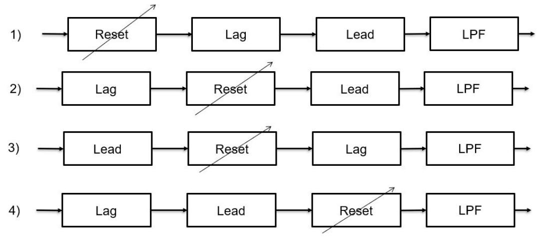

Fig. 18: Possible sequence of filters

VIII. Zero Crossings

The concept of reset control is based on the number of resets and their instants. When the input signal to the controller crosses the zero line, the controller resets. The number of resets directly correlates to the nonlinearity present in the output. Ideally, two resets are desired in one period of input as seen from the Fig. 1.In reality, the resets are not triggered from the reference signal but from the error signal, Fig. 2.

If the error signal consists dominantly of the reference frequency, then the prediction of the output of controller is accurate. But, if the error signal consists of more than one frequency causing multiple resets (zero crossings), the prediction of the output of the controller is difficult. For instance, for Bandpass CGLP (for specification refer [26]) with a reference of 10 Hz the error plot is shown in Fig. 19a. It can be seen that the controller is resetting 6 times in one period of input. The out of the controller is shown in Fig. 19b. It is clear that the controller does not follow there error signal, rather it consists of higher frequencies. In such a case if we include a disturbance then we cannot predict the output of the system accurately as the superposition principle is not valid. To predict the output of reset element in closed-loop, excessive resets should be avoided.

$$y = Asin(\alpha t + \theta) + Bsin(\beta t + \phi) \tag{25}$$

In [30], superposition of two sinusoids as shown in Eq. 25 is discussed. The number of times the output '$y(t)$' crosses the zero line depends on the amplitude, frequency and in certain cases on phase. For instance, in equation Fig. 25 if $A > B$ and $\alpha > \beta$, then the output will follow the α and will same number of zero crossings as that of $A\sin(\alpha t + \theta)$ irrespective of what phase they have. In our case, the first harmonic has a higher amplitude but the 3^{rd} harmonic has a higher frequency, that is $A > B$ and $\alpha < \beta$, the zero-crossing of 'y' depends on the phases θ and ϕ as well. Therefore, to avoid multiple resets we have to take into account both the amplitude and phase of higher-order harmonics.

IX. Thesis Objective and Conclusion

The recently developed structure for the single state reset elements to bandpass the nonlinearity needs further study. The effect of band length, band shape, band depth and position of the band on superposition principle, tracking, settling time, overshoot and noise rejection needs investigation. As discussed in section V the parameters ψ and γ can be tuned for the same phase margin with different higher-order harmonics.

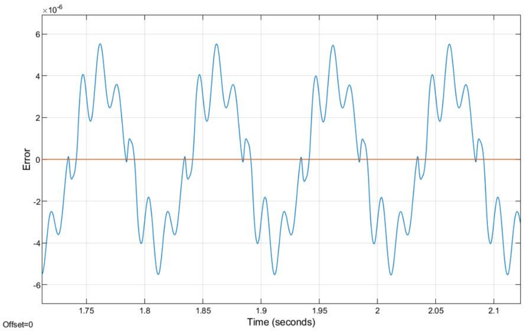

(a) Closed loop error

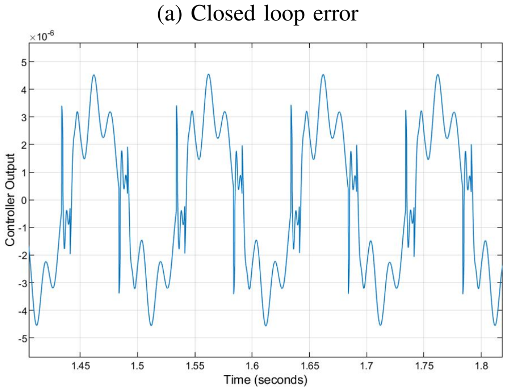

(b) Controller output

Fig. 19: Effect of multiple resets on the controller output

The main goal of this research is to find a threshold limit for the magnitude and phase of higher-order harmonics for avoiding excessive resets. After finding the limits for higher-order harmonics, the next step is to determine whether can we achieve those magnitudes and phase. We have tools in the form shaping filter, ψ, γ and other filters like K, T in the bandpass CGLP to influence the magnitude and phase of first and higher-order harmonics. All the closed-loop methods have an assumption number of resets (two) in one period of input. Finding a threshold cap for higher-order harmonics such that resets are caused only by first harmonics and not by the higher ones. Such an investigation can help improve the closed-loop analysis of the reset system.

Reset control provides an edge over the limitation of linear control. Both broadband and narrowband phase compensation can be achieved using reset elements like FORE, CGLP and bandpass CGLP. Reset control has its drawbacks of superposition being not valid, generation of higher-order harmonics (unwanted), dependency on the gain, etc. These nonlinear effects make analytical closed-loop analysis complex and not accurate. Tipping the balance of reset systems away from the nonlinear effects while utilising the phase advantage is the main theme.

References

[1] R. M. Schmidt, G. Schitter, and A. Rankers, *The Design of High Performance Mechatronics-: High-Tech Functionality by Multidisciplinary System Integration*. Ios Press, 2020.

[2] J. Clegg, "A nonlinear integrator for servomechanisms," *Transactions of the American Institute of Electrical Engineers, Part II: Applications and Industry*, vol. 77, no. 1, pp. 41–42, 1958.

[3] I. Horowitz and P. Rosenbaum, "Non-linear design for cost of feedback reduction in systems with large parameter uncertainty," *International Journal of Control*, vol. 21, no. 6, pp. 977–1001, 1975.

[4] L. Hazeleger, M. Heertjes, and H. Nijmeijer, "Second-order reset elements for stage control design," in *2016 American Control Conference (ACC)*. IEEE, 2016, pp. 2643–2648.

[5] N. Saikumar, R. K. Sinha, and S. H. HosseinNia, "“constant in gain lead in phase” element–application in precision motion control," *IEEE/ASME Transactions on Mechatronics*, vol. 24, no. 3, pp. 1176–1185, 2019.

[6] N. Karbasizadeh, N. Saikumar, and S. H. HosseinNia, "Fractional-order single state reset element," *arXiv preprint arXiv:2009.11131*, 2020.

[7] A. Vidal and A. Baños, "Reset compensation for temperature control: Experimental application on heat exchangers," *Chemical Engineering Journal*, vol. 159, no. 1-3, pp. 170–181, 2010.

[8] V. Ghaffari, P. Karimaghaee, and A. Khayatian, "Reset law design based on robust model predictive strategy for uncertain systems," *Journal of Process Control*, vol. 24, no. 1, pp. 261–268, 2014.

[9] E. Akyüz, N. Saikumar, and S. H. HosseinNia, "Reset control for vibration disturbance rejection," *IFAC-PapersOnLine*, vol. 52, no. 15, pp. 525–530, 2019.

[10] A. Baños and A. Vidal, "Definition and tuning of a pi+ ci reset controller," in *2007 European Control Conference (ECC)*. IEEE, 2007, pp. 4792–4798.

[11] L. Zaccarian, D. Nesic, and A. R. Teel, "Set-point stabilization of siso linear systems using first order reset elements," in *2007 American Control Conference*. IEEE, 2007, pp. 5808–5809.

[12] M. Ivens, "Robust reset control using adaptive/iterative learning control," 2018.

[13] Y. Guo, L. Xie, and Y. Wang, *Analysis and design of reset control systems*. Institution of Engineering and Technology, 2015.

[14] A. Vidal and A. Banos, "Qft-based design of pi+ ci reset compensators: application in process control," in *2008 16th Mediterranean Conference on Control and Automation*. IEEE, 2008, pp. 806–811.

[15] D. Rijlaarsdam, P. Nuij, J. Schoukens, and M. Steinbuch, "A comparative overview of frequency domain methods for nonlinear systems," *Mechatronics*, vol. 42, pp. 11–24, 2017.

[16] Y. Li, G. Guo, and Y. Wang, "Nonlinear mid-frequency disturbance compensation in hard disk drives," *IFAC Proceedings Volumes*, vol. 38, no. 1, pp. 31–36, 2005.

[17] Y. Guo, Y. Wang, and L. Xie, "Frequency-domain properties of reset systems with application in hard-disk-drive systems," *IEEE Transactions on Control Systems Technology*, vol. 17, no. 6, pp. 1446–1453, 2009.

[18] P. Nuij, O. Bosgra, and M. Steinbuch, "Higher-order sinusoidal input describing functions for the analysis of non-linear systems with harmonic responses," *Mechanical Systems and Signal Processing*, vol. 20, no. 8, pp. 1883–1904, 2006.

[19] K. Heinen, "Frequency analysis of reset systems containing a clegg integrator: An introduction to higher order sinusoidal input describing functions," 2018.

[20] O. Beker, C. Hollot, Y. Chait, and H. Han, "Fundamental properties of reset control systems," *Automatica*, vol. 40, no. 6, pp. 905–915, 2004.

[21] Y. Salman, "Tuning a novel reset element through describing function and hosidf analysis," 2018.

[22] X. Hou, A. A. Dastjerdi, N. Saikumar, and S. H. HosseinNia, "Tuning of constant in gain lead in phase (cglp) reset controller using higher-order sinusoidal input describing function (hosidf)," *arXiv preprint arXiv:2009.05116*, 2020.

[23] N. Karbasizadeh, A. A. Dastjerdi, N. Saikumar, D. Valerio, and S. H. HosseinNia, "Benefiting from linear behaviour of a nonlinear reset-based element at certain frequencies," *arXiv preprint arXiv:2004.03529*, 2020.

[24] L. van Duist, G. van der Gugten, D. Toten, N. Saikumar, and H. HosseinNia, "Flores-fractional order loop shaping matlab toolbox," *IFAC-PapersOnLine*, vol. 51, no. 4, pp. 545–550, 2018.

[25] A. Oustaloup, *La commande CRONE: commande robuste d'ordre non entier*, 1991.

[26] N. Karbasizadeh, A. A. Dastjerdi, N. Saikumar, and S. H. HosseinNia, "Band-passing nonlinearity in reset elements," *arXiv preprint arXiv:2009.06091*, 2020.

[27] N. Saikumar, K. Heinen, and S. H. HosseinNia, "Loop-shaping for reset control systems–a higher-order sinusoidal-input describing functions approach," *arXiv preprint arXiv:2008.10908*, 2020.

[28] R. Buitenhuis, N. Saikumar, and S. HosseinNia, "Frequency-domain modelling of reset control systems using an impulsive description," *arXiv preprint arXiv:2009.13341*, 2020.

[29] C. Cai, A. A. Dastjerdi, N. Saikumar, and S. H. HosseinNia, "The optimal sequence for reset controllers," *arXiv preprint arXiv:2005.13877*, 2020.

[30] N. Blachman, “Zero-crossing rate for the sum of two sinusoids or a signal plus noise (corresp.),” *IEEE Transactions on Information Theory*, vol. 21, no. 6, pp. 671–675, 1975.

3 Problem statement

3.1 Problem definition

The literature study indicates the potential of reset elements to boost the performance of linear control. With the additional phase provided by the reset elements, transient response, robustness and stability can be improved without compromising precision. Every new technology in the world is an improvement over the previous generation but comes with some downsides. Similarly, the phase advantage comes at an expense of higher-order harmonics. These high order harmonics have a small magnitude in an open loop. But in closed-loop, the higher-order harmonics are fed back to the controller and are amplified in magnitude. These can then excite higher frequency modes of a multimodal system.

In a linear system, ideally any frequency up to bandwidth can be used as reference. In reset systems, so is not the case due to the higher-order harmonics in the feedback loop. Usually, a reference below 1.5 to 2 order of bandwidth is used for tracking. In this frequency range, a well-tuned reset closed-loop system can be predicted for certain references, being the only input. Any other reference outside that range can produce higher-order harmonics with significant magnitude. For instance, if a CGLP with a cutoff frequency close to linear integrator cutoff frequency, any reference near this cutoff can result in high nonlinearity. Another issue with nonlinear systems is the superposition principle being invalid. Even if there is known disturbance and noise in the system, still it is difficult to estimate the closed-loop response with multiple inputs. There is no direct relation between open-loop and closed-loop performance. To determine how and which higher-order harmonic will be dominant in closed-loop is difficult to estimate.

As discussed in the literature, numerical and analytical methods have been recently introduced to estimate closed-loop sensitivities. All these methods come with some assumptions, of which one is having only two resets (zero crossings) in the signal input to the reset element in one period of reference frequency. Also, the instants at which these zero-crossings occur is of significance. If there are more than two resets then the analytical closed-loop estimation is not accurate. These multiple zero crossings are caused by higher harmonics of the reference signal. If the multiple zero crossings are well separated (on the time axis) in one period of input frequency, then the higher harmonics are more dominant. But again there is no way to determine which harmonics are responsible for these multiple zero crossings through the analytical open-loop or closed-loop analysis and further how can they be suppressed.

A solution to the above problem is to inherently avoid multiple zero crossings by tuning the controller to have low higher-order harmonics. This brings us to the main question of this thesis: "How low should be the higher-order harmonics to avoid excessive zero crossings in the reset signal?" or imperatively **"Avoiding excessive zero crossings in reset control"**.

3.2 Research objectives

To find an amplitude threshold on higher-order harmonics to avoid multiple zero crossings, consider a closed-loop system with reset and linear controllers. Consider the signal input to reset element is a sum of sinusoidal higher order harmonics with amplitude A_n and phase θ_n, where 'n' is the index of higher harmonics. The research objectives to be looked upon are:

1. To find the number of odd higher harmonics (n) to be taken into account
2. The phase θ_n that cause multiple zero crossings with lowest possible amplitude of higher-order harmonic
3. To find amplitude distribution A_n by computing closed-loop sensitivity using open-loop HOSIDF estimation
4. To calculate the ideal input to reset element (the threshold for higher-order harmonics)

5. To map the closed-loop threshold to open-loop
6. To tune a controller to satisfy the threshold for an actual plant
7. To validate the amplitude threshold theory by inspection of zero crossings through time-domain simulation

4 Avoiding excessive zero crossings in reset control

This chapter presents a paper on avoiding excessive resets in reset control. The paper initiates with a general introduction to linear and reset control. Section II reviews the basics of reset control, its state-space formulation and the frequency domain response of reset elements using Higher Order Sinusoidal Input Describing Functions (HOSIDF). Section II presents frequency domain response of reset elements like FORE and CGLP along with open-loop HOSIDF based closed-loop approximation. Section III presents the theory on how to avoid multiple zero crossings (resets) for a multi-sine sinusoidal signal with odd higher harmonics. This section discusses the phase for multiple reset, amplitude distribution of higher-order harmonics, mapping from closed-loop to open-loop, steps to calculate the amplitude threshold. Section IV illustrates an example to validate the theory in section III. Last, section V provides the conclusion and recommendations.

Avoiding excessive zero crossings in reset control

Shrinath Diwakar, Nima Karbasizadeh, S. Hassan HosseinNia

***Abstract*—This paper presents criteria to avoid excessive zero-crossings caused by odd higher-order harmonics in a multi-sine signal. This criterion can be used in the field of reset control. Reset control overcomes the drawbacks of linear control like Bode gain phase relation and waterbed effect. Reset elements like CGLP, FOSRE, etc can provide a phase lead with constant magnitude behaviour. The main drawback of reset elements is the generation of higher-order harmonics. The number zero-crossings influences the closed-loop performance of a signal input to the reset element. Due to higher-order harmonics, multiple resets can occur, which makes the close loop analysis becomes complex. The criteria to avoid excessive zero-crossings provides a threshold on the amplitude of higher-order harmonics. This criterion is validated by a time-domain analysis of a CGLP reset architecture.**

***Index Terms*—Mechatronics, motion control, precision control, reset control, nonlinear control.**

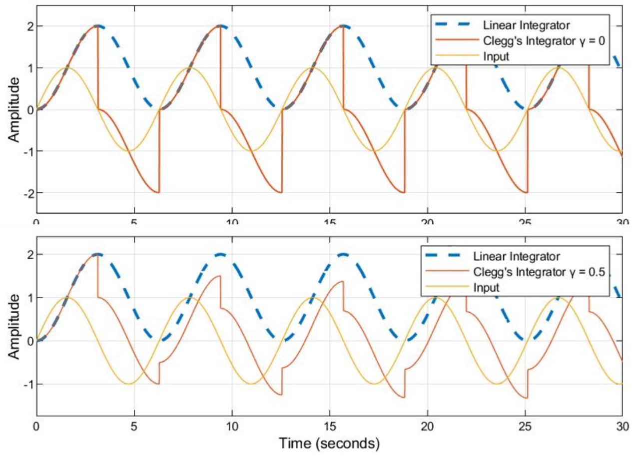

Fig. 1: Simulation of Clegg's Integrator

I. Introduction

The world is moving towards miniaturization every day. Electronic circuits are getting smaller and more power-efficient. The smartphone processors are developed on a scale of 5nm to date. The sensors used in automobiles, heavy machinery, etc are moving towards nano-meter scale. To sustain this progress, we need machines that are cable of moving and sensing small movements. For doing so control systems play an important role, especially PID controllers. PID controllers have been used in the industry for about a century. PIDs cover the majority share of the various controllers available to the industry. The reason behind this is the ease of implementability and tunability. The analysis of PIDs in the frequency domain paves the way to capture more information of the modes and system behaviour at a wide range of frequencies.

Linear controllers come with limitation like Bode gain phase relation. Ideally, high bandwidth is desired and a phase lead around bandwidth to assure system stability. Improving the tracking performance can be done by increasing the gain at lower frequencies. Doing so results in phase reduction at the bandwidth. As a result, system tracking and robustness contradict each other. In other words, if one improves other degrades. Another limitation of PID is the Waterbed effect [1], where improving performance at one frequency will degrade the performance other frequency. There are other limitations like integral windup and saturation as well. Due to all these limitations, PID cannot be used to achieve all the system requirements.

To overcome the limitations of linear control, nonlinear control theory is used. Reset control is a branch of nonlinear controllers which is becoming popular. A rest controller resets its state/ states to a certain value when a certain condition is met. Doing so reduces the phase lag, keeping the same gain characteristics. Nonlinear systems are generally analysed in the time domain which makes the implementation difficult in practice. Describing function analysis is used to transform the time domain study into frequency domain approximation, which eases the implementation with the loop shaping method. In the late 1950s, JC Clegg introduced the first reset element as Clegg's Integrator (CI) [2]. The time-domain response of a linear integrator (LI) and CI is compared in Fig. 1. The CI resets its output when the input signal crosses the x-axis. The reset value in Fig. 1 (upper sub-figure) is set to zero but it can vary anywhere between its positive and negative amplitude span. This resetting action provides a maximum phase advantage of 52° over the LI. The gain of CI has the same slope as LI but a slightly high gain. This idea of CI was further used to develop many other resets elements namely First Order Reset Element (FORE) [3], Second Order Reset Element (SORE) [4], Constant Gain Lead Phase (CGLP) [5], Fractional Order Single State Reset element (FOSRE) [6], etc. These elements have similar magnitude characteristics but different phase behaviour as compared to linear lead and bandpass pass filters.

Reset controllers (RC) are broadly used as wide-band phase compensators. As discussed earlier, RC provides phase lead with zero gain behaviour and thus increase the phase margin available at the bandwidth. The rise time and overshoot performance are improved as well. Many engineering domains have utilised RC for improving the performance, thermal [7], chemical [8], vibration control [9], precision motion control [5]. The reset controllers have a downside as well. In the Fig. 1, at reset instants there is a sudden jump in the state of the controller. Hence, adding a high degree of nonlinearity into the system and thus higher-order harmonics in the output.

The structural outline of this paper is as follows; Section

II captures preliminaries of reset control and zero crossings. Section III discusses the effect of multiple zero crossings on CGLP and provides amplitude threshold criteria to avoid these multiple zero crossings. Section IV provides an example to validate the theory followed by the conclusion.

II. Preliminaries of reset control

A. State Space formulation

The Eq. 1 represents a generalised state space formulation of a reset controller (RC) [10]. A, B, C, D are state matrices of the RC. A_ρ represents the reset matrix. When the input $e(t) = 0$, the current states $x(t)$ gets resets to certain value according to A_ρ. If $e(t) \neq 0$, the state space follows the base linear form for the RC.

$$\sum\nolimits_R = \begin{cases} \dot{x}_r(t) = Ax_r(t) + Be(t) & \text{if } e(t) \neq 0, \\ x_r(t^+) = A_\rho x_r(t) & \text{if } e(t) = 0, \\ u(t) = Cx_r(t) + De(t) \end{cases} \tag{1}$$

In the above case, the reset condition is set to zero crossings of input $e(t)$ but that can be altered. Other reset laws like reset band can be found in [11] [7] where, if the input $e(t)$ is in a certain band the reset is triggered.

B. Stability analysis

In linear systems, the stability can be checked from the Nyquist plot or by checking phase ($> 180°$) at bandwidth and gain (> 0) at zero phase crossing. If these criteria are fulfilled the system is BIBO stable. For the implementation of reset elements, first, the base linear system should be BIBO stable. To inspect the quadratic stability H_β condition should be fulfilled [12] [10].

Theorem 1. *There exist a $\beta \in \Re^{n_r \times 1}$ and positive definite matrix $P_\rho \in \Re^{n_r \times n_r}$, such that the restricted Lyapunov equation*

$$P > 0, \; A_{cl}^T P + P A_{cl} < 0 \tag{2}$$

$$B_0^T P = C_0 \tag{3}$$

has a solution for P, where

$$C_0 = \begin{bmatrix} \beta C_p & 0_{n_r \times n_{nr}} & P_\rho \end{bmatrix}, B_0 = \begin{bmatrix} 0_{n_p \times n_r} \\ 0_{n_{nr} \times n_r} I_{nr} \end{bmatrix} \tag{4}$$

and,

$$A_\rho P_\rho A_\rho - P_\rho \leq 0 \tag{5}$$

A_p, B_p, C_p, D_p are state matrices of the plant, A_{cl} is the closed-loop (controller and plant) state A matrix. n_r are the number of states being reset, n_{nr} are states not being reset and n_p are the number of states of a plant.

There exist a $\beta \in \Re^{n_r \times 1}$ and positive definite matrix $P_\rho \in \Re^{n_r \times n_r}$, such that the restricted Lyapunov equation

$$P > 0, \; A_{cl}^T P + P A_{cl} < 0 \tag{6}$$

$$B_0^T P = C_0 \tag{7}$$

has a solution for P, where

$$C_0 = \begin{bmatrix} \beta C_p & 0_{n_r \times n_{nr}} & P_\rho \end{bmatrix}, B_0 = \begin{bmatrix} 0_{n_p \times n_r} \\ 0_{n_{nr} \times n_r} I_{nr} \end{bmatrix} \tag{8}$$

and,

$$A_\rho P_\rho A_\rho - P_\rho \leq 0 \tag{9}$$

A_p, B_p, C_p, D_p are state matrices of the plant, A_{cl} is the closed-loop (controller and plant) state A matrix. n_r are the number of states being reset, n_{nr} are states not being reset and n_p are the number of states of a plant.

C. Describing functions

The Describing Function (DF) is used to approximate the steady-state output of a nonlinear in the time domain to the frequency domain. This approximation is made by the Fourier series by using only the first fundamental frequency. If the input is sinusoidal, the DF becomes Sinusoidal Input DF (SIDF). Guo et al. in [13] and [14], presented a SIDF analysis for reset systems with input $e(t) = 0$ as the reset instants.

For nonlinear systems, for an input of a certain frequency, the output will have higher-order harmonics of input frequency having with different individual amplitude and phase. [15]. The SIDF only encapsulates the input gain dependent non-linear effect and not the others. Along with this, DF analysis does not provide any gain-phase information of frequencies not present in the input. Therefore, SIDF analysis is not accurate enough to approximate a reset system. Heinen et al. [16], extended the DF analysis in [14] and presented HOSIDF. HOSIDF approximates the reset system using Fourier series with higher frequencies included. The Eq. 10 presents the HOSIDF expression for reset systems with A, B, C, D as its state matrices and n in represents the harmonic number.

$$H_n(\omega) = \begin{cases} C(j\omega I - A)^{-1}(I + j\Theta(\omega))B + D & n = 1 \\ C(j\omega n I - A)^{-1} j\Theta(\omega)B & n_{odd} > 2 \\ 0 & n_{even} \geq 2 \end{cases} \tag{10}$$

where,

$$\begin{aligned} \Theta_D(\omega) &= \frac{-2\omega^2}{\pi} \triangle(\omega)[\Gamma_r(\omega) - \Lambda^{-1}(\omega)] \\ \Lambda(\omega) &= \omega^2 I + A^2 \\ \triangle(\omega) &= I + e^{\frac{\pi}{\omega}A} \\ \triangle_r(\omega) &= I + A_\rho e^{\frac{\pi}{\omega}A} \\ \Gamma_r(\omega) &= \triangle_r^{-1}(\omega) A_\rho \triangle(\omega) \Lambda^{-1}(\omega) \end{aligned} \tag{11}$$

D. FORE

Taking Clegg's integrator ahead, Horowitz et al. in [3] introduced the First Order Reset element (FORE). FORE is a reset version of a linear first-order low pass filter (LPF). The Eq. 12 shows the analytical expression of FORE with w_r as the corner frequency. In the Fig. 2 the frequency response of FORE is shown with a corner frequency of 5 Hz along with higher-order harmonics. The first harmonic phase of FORE tends to $-38°$ at high frequencies. The higher-order harmonics are most dominant around corner frequency.

GFORE [14] has two variables w_r and $A_\rho = \gamma$, where $\gamma \in (-1, 1)$. Varying the γ affects the phase advantage and dominance of higher-order harmonics. For $\gamma = 1$, the filter has no non-linearity has behaves like a linear LPF.

$$FORE = \cancelto{A_\rho}{\frac{1}{s/\omega_r + 1}} \tag{12}$$

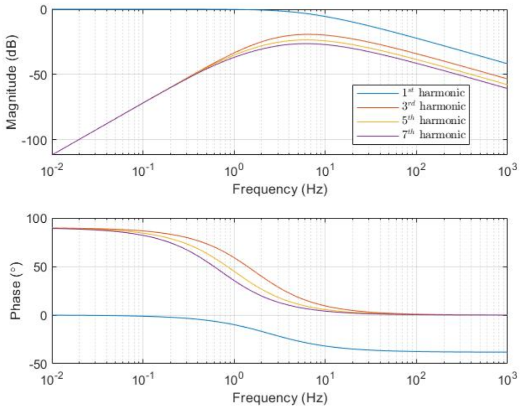

Fig. 2: Frequency response of FORE for $w_r = 5$ Hz and $\gamma = 0$

E. CGLP

Constant in Gain Lead in Phase (CGLP) is a reset element recently developed by Saikumar et al. [5]. GGLP provides phase lead over a range of frequencies with a constant gain behaviour. This element is an alternative to the lead filter in PID. Using GFORE in series with a corresponding order lead filter forms a CGLP. The analytical expression of first-order CGLP is shown in Eq. 13 with w_r and w_f as the range in which phase lead is obtained. Due to resetting action, a shift in the corner frequency of FORE is observed. To compensate for this shift, a variable α is introduced as $w_r = \alpha\, w_{r\alpha}$.

$$CGLP = \cancelto{A_\rho}{\frac{1}{\frac{s}{\omega_{r\alpha}} + 1}} \; \frac{s/\omega_r + 1}{s/\omega_f + 1} \tag{13}$$

F. Closed loop analysis of reset system

In linear control, the closed-loop performance can be estimated accurately with an open-loop, so this is not the case with reset control. The reset element outputs odd higher-order harmonics of a reference frequency. All these higher harmonics are fed back to the controller in the closed-loop. This makes closed-loop estimation difficult from the open-loop response.

To estimate the performance of a Closed-Loop Reset System (CLRS), numerical methods [17] have been applied by Dastjerdi et al., which provide close to real results. Such numerical calculations are computationally expensive and do not provide any information about the system dynamics as the analysis is in the time domain. Recently, Saikumar et al. presented an analytical method to estimate the CLRS from the open-loop [18]. The reset system is modelled as a harmonic generator that produces higher harmonics for a reference frequency. The Eq. 14 and 15 represents analytical expressions to estimate the closed-loop sensitivity (S_n) for a architecture shown in Fig.4. The subscript bl stands for base-linear system, where the reset element has $\gamma = 1$. Accordingly, $L_{bl}(\omega)$ and $S_{bl}(\omega)$ are the open-loop and closed-loop sensitivity function of base linear systems respectively. $L_n(\omega)$ is the open loop HOSIDF function where $H_n(\omega)$ is the reset element. This analytical method provides accurate results in the region where the higher-order harmonics are not dominant.

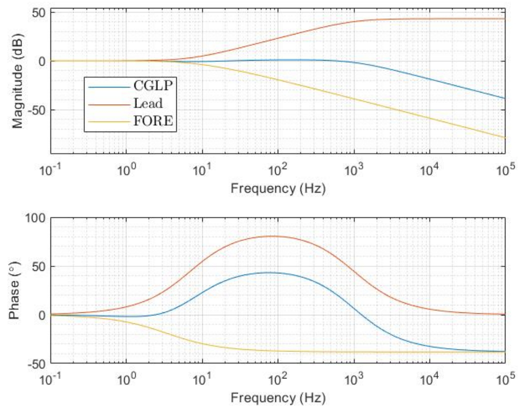

Fig. 3: Frequency response of CGLP for $w_{r\alpha} = 5$ Hz, $\gamma = 0$, $\omega_f = 1000$ Hz and $\alpha = 1.4$

$$S_1(\omega) = Sl_1(\omega) \tag{14}$$

$$S_{n>2}(\omega) = \left(\frac{L_n(\omega)}{C_1(\omega)}\right) S_{bl}(n\omega) |C_1 S_1| \angle(n(C_1 S_1)) \tag{15}$$

where,

$$\begin{aligned} L_n(\omega) &= C_1(\omega)\, H_n(\omega)\, C_2(n\omega)\, P(n\omega) \\ Sl_n(\omega) &= \frac{1}{1 + L_n(\omega)} \\ L_{bl}(\omega) &= C_1(\omega)\, R_{bl}(\omega)\, C_2(\omega)\, P(\omega) \\ S_{bl}(\omega) &= \frac{1}{1 + L_{bl}(\omega)} \end{aligned} \tag{16}$$

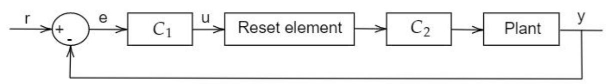

Fig. 4: Closed loop architecture with C_1 and C_2 as linear elements

An illustrative example of closed-loop sensitivity for a reset system is shown in Fig. 5. The architecture in Fig. 4 is followed with Eq. 17 as controllers. The filters are designed for a bandwidth of 100 Hz. In the Fig. 5, response till 11^{th}

harmonic is shown. The plant has the resonance at 2.5 Hz where all the higher harmonics show a zero like behaviour. In the range 5 Hz to 100 Hz, many higher harmonics have a peak like behaviour. These peaks can result in multiple resets and poor prediction of error will not be accurate. We can also see the decaying behaviour of higher harmonics with a -2 slope. The cutoff frequency for these higher harmonics gets lower as the count of harmonic increases.

$$\begin{aligned} C_1 &= 1 \\ H_n = CGLP &= \cancelto{A_\rho}{\frac{1}{\frac{s}{\omega_{r\alpha}}+1}} \quad \frac{s/\omega_r+1}{s/\omega_f+1} \\ C_2 &= k_p\left(1+\frac{\omega_i}{s}\right)\left(\frac{s/\omega_d+1}{s/\omega_t+1}\right)\left(\frac{1}{s+w_f}\right)^2 \\ Plant\ (P(s)) &= \frac{3.038\,e04}{s^2+0.7413\,s+243.3} \end{aligned} \tag{17}$$

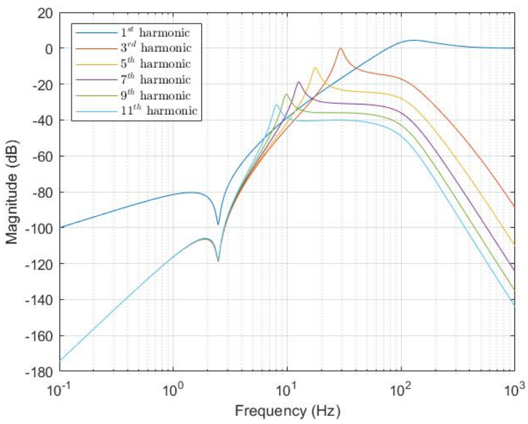

Fig. 5: Closed-loop Sensitivity for the control scheme shown in the Eq. 17

G. *Sequence of filters in reset control*

In linear systems, the order of filters like lead, lag and plant does not change the output in open-loop and closed-loop. Any combination will result in the same output. In the reset systems as superposition does not hold and different order provides different results. The Fig. 6 shows the possible sequences of lead, lag, reset with a low pass filter (LPF) is shown. In the open-loop, all the sequences provide the same result but in the closed-loop different sequence provide a different result. Cai et al. proposed an optimal order for these possible combinations in [19]. Sequence 3 is the optimal sequence if there is a low ratio of noise to input amplitude. If there is noise in the system, sequence 1 works best as the lag filter just after the reset systems act like an LPF for higher-order harmonics. The LPF being a lag filter should always be placed after reset so that the higher harmonics can be attenuated for best results. Later in the report, an example is provided which utilises sequence 3.

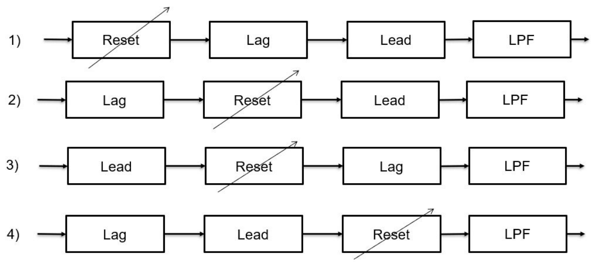

Fig. 6: Possible sequence of filters

H. *Zero crossings*

In [20], Blachman presents a superposition of two sinusoids as shown in Eq. 18 is discussed. The number of times the output $y(t)$ crosses the zero line depends on the amplitude, frequency and in certain cases on phase. For instance, in Eq. 18 if $A > B$ and $\alpha > \beta$, then the output will follow the α and will the same number of zero crossings as that of $A\sin(\alpha t + \theta)$ irrespective of what second sinusoid. In the case of reset elements, the first harmonic has a higher amplitude but the 3^{rd} harmonic has a higher frequency, that is $A > B$ and $\alpha < \beta$, the zero-crossing of $y(t)$ depends on the phases θ and ϕ as well. Therefore, to avoid multiple zero crossings we have to consider both the amplitude and phase of higher-order harmonics.

$$y = Asin(\alpha t + \theta) + Bsin(\beta t + \phi) \tag{18}$$

III. Avoiding excessive zero crossings

A. *Superposition of Higher Harmonics*

The superposition principle holds if the law of additivity and law of homogeneity are satisfied. From the above discussion, we know that the reset element results in odd higher harmonics in the output for an input frequency. In the Fig. 7, $\theta_{out} = f(\theta, 3\theta, 5\theta, ...)$ and $\alpha_{out} = f(\alpha, 3\alpha, 5\alpha, ...)$. In a closed-loop system, these higher harmonics will be fed back to the reset element as input. This will create a multi-sine input to the reset element, that is θ and α will consist of higher harmonics. The law of additivity as shown in Fig. 7 (reset system 3) will hold only if $\theta, \alpha, \theta_{out}$ and α_{out} will consist dominantly of its fundamental frequency. The law of homogeneity holds for reset elements as they are linear in gain.

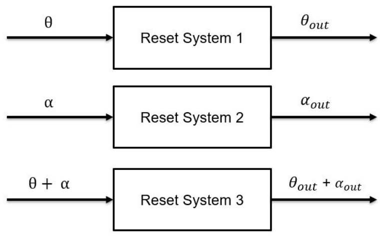

Fig. 7: Superposition for reset element

B. Effect of multiple resets / zero crossings

The reset law defines the instance of resets. The reset law followed in the Clegg's integrator is by the zero crossings of the reference frequency. In one period of input, the signal crosses the zero line twice, which is the ideal case. In a closed-loop system, the input to the reset element is never the reference signal. The input to the reset element is often a multi-sine signal. The Fig. 8 shows such a case, where the input to the controller has multiple zero crossings in one period of the reference. The output of the controller consists of different frequencies compared to input. In such cases, where the superposition principle is not valid, predicting the closed-loop performance with disturbance and noise is difficult. Another issue is the missing link between the open-loop and closed-loop. There is no way to predict these multiple zero crossings in a closed-loop from the open-loop response. Therefore, to tune the system we to need to compute the closed-loop response repeatedly, which is computationally expensive.

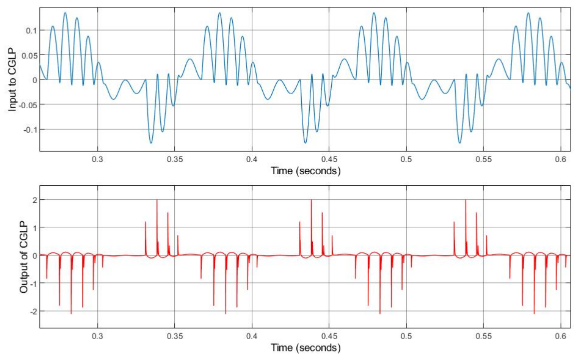

Fig. 8: Time response of the architecture shown in 4 with $C_1 = 1$, reset element as FORE CGLP, C_2 as PID and 2^{nd} order LPF

The input signal to a reset controller can be analytically expressed as in Eq. 19. As discussed in the zero crossings section, the zero crossings is the function of amplitude A_n and phase ϕ_n. To find the optimum conditions for multiple zero resets, A_n and ϕ_n needs to be approximated which is discussed in the next section.

$$u = A_n \sum_{n=1}^{m} \sin\left(n\omega t + \theta_n\right) \tag{19}$$

where, $n \in odd\ N$

C. Phase of higher order harmonics for multiple resets

To have multiple zero crossings, the higher harmonics should interfere destructively near zero crossings of the first harmonic. The slope of the first harmonic and higher harmonics should be of opposite sign near zero crossings. The Eq. 20 presents a phase relation for higher harmonics for destructive interference with the first harmonic. An illustrative example is shown in Fig. 9, where the third and fifth harmonic intersect exactly at zero crossings of the first harmonic but with opposite slope. The phase for multiple resets (θ_n) provides an optimum phase such that the lowest possible amplitude of higher harmonics which can cause reset, can be found. If we have amplitude higher than this given least possible value we have a buffer zone in phase around θ_n. In the Fig. 9, the phase of the third and fifth harmonic can be shifted around θ_n and still result in multiple reset as their combined amplitude is higher than the least possible amplitude. This shift around θ_n depends on how high the combined amplitude of higher harmonics is.

$$\theta_n = \left(\theta_1 - \pi/n\right) n \tag{20}$$

where, $n \in odd\ N \geq 3$ and θ_1 is the first harmonic phase

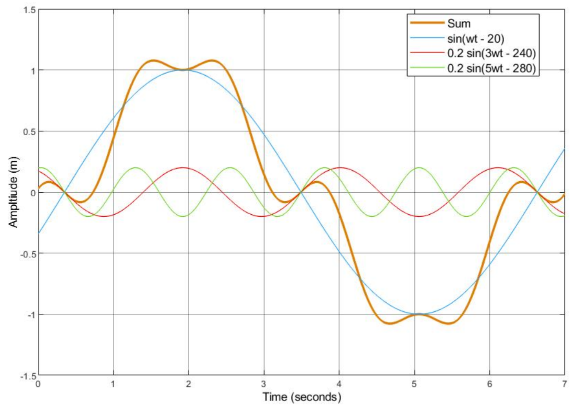

Fig. 9: Phase of higher order harmonics for multiple resets

D. Amplitude distribution of higher order harmonics

In the Eq. 19, the amplitude A_n $(n \geq 3)$ is the analytical distribution. The analytical amplitude distribution uses Eq. 15 to calculate transfer function from u to r. Later the higher harmonics are normalised by third harmonic as shown in Eq. 22 for a certain frequency ω. This amplitude distribution is unique for every cutoff frequency ω_r and γ, as varying the these parameters will the magnitude of higher harmonics for a frequency. But this change in relative magnitude is not significant enough. Hence, computing the amplitude distribution for a set of ω_r and γ and using the same amplitude distribution for tuning the reset element is a good approximation.

The Fig. 10 shows how the relative amplitudes vary with respect to third harmonic for 1 Hz, 20 Hz and 50 Hz. For the lower frequencies, the amplitude does not vary rapidly with an increase in the harmonic count. Therefore, more number of harmonics should be taken into account for this region. While for the higher frequencies the case is opposite. Within a couple of hundred harmonics, the amplitude difference drops to five orders less. The number of harmonics to be considered also depends on the sampling frequency. For lower frequency, the number of harmonics to be considered is when the amplitude drops to 4 order (-80 dB) or less. Usually this number is somewhere between 1000 to 5000 odd harmonics. For higher frequencies, considering 100 to 1000 odd harmonics is a good approximation. More discussion on this section is presented in appendix C and D.

$$I_n^{'} = \frac{u}{r} = \frac{C_1(n\omega)\,e}{r} = C_1(n\omega)\,S_n \tag{21}$$

where, S_n is closed loop sensitivity

$$A_n(n\omega) = k_{gain}|(I_n^{'}/I_3^{'})_\omega| \tag{22}$$

where, $n \in odd\,N \geq 5$, $k_{gain} \in R \leq 0$

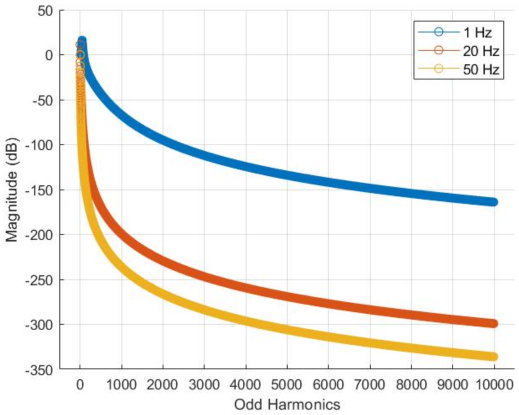

Fig. 10: Analytical higher order harmonics amplitude distribution normalised by 3^{rd} harmonic for the control scheme shown in Eq. 17

E. Ideal normalised input to the reset element

In the Eq. 19, we now have data for both variables amplitude and phase. Now we select a frequency, input the first harmonic phase and sum the sinusoids as represented in equation 19. As the third harmonic is the datum point for the higher harmonics, changing the datum point along with the y-axis (dB) we can check for the multiple resets. The figure 11 shows ideal sensitivity normalised by first harmonic for the control scheme as in equation 17. The Fig. 11 is analytically expressed as I_ω^* in Eq. 23. Various frequencies between 1 Hz to 100 Hz (bandwidth) are selected (Fig. 11) for which the amplitude threshold of higher harmonics is calculated. These threshold values vary with the step size. Lower the step size, higher frequencies can be detected and hence, summed in Eq. 19. We can see that for lower frequencies the amplitude limit is about -90 dB as the in this region harmonics are densely packed. As the frequency increases, the amplitude limit gets higher because the higher harmonics start to decay with second-order slope.

$$I_\omega^* = \frac{\sum_n^m |(I_n^{'})_\omega|}{|(I_1^{'})_\omega|} \tag{23}$$

where, $n \in odd\,N \geq 3$

F. Mapping from closed loop to open loop

We can check whether the controller satisfies the amplitude threshold from the previous section and by calculating Eq. 23 using Eq. 22. But calculating equation 22 repeatedly is computationally expensive. To reduce this computation cost, two steps are proposed; first to map the closed-loop sensitivity

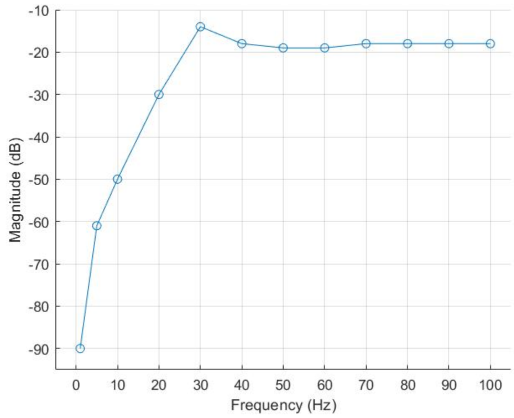

Fig. 11: Ideal input to the reset element normalised by first harmonic (I_ω^*) for the architecture in the Fig. 4 and Eq. 17

to the open loop. Second, using only the third harmonic instead of the sum of all higher harmonics as shown in Eq. 23. The Eq. 24 represents the analytical expression for such a mapping. If the normalised third harmonic open-loop follows the threshold then the other higher will also follow the same. The aim is to bring the normalised open-loop below the threshold.

$$\left(\frac{L_3}{L_1}\right)_\omega = \left(\frac{I_3}{I_1}\right)_\omega \frac{-C_1^2}{C_1(3\omega)Sl_{bl}(3\omega)L_1(1+L_1)|C_1S_1|} \tag{24}$$

where,

$$\left(\frac{I_3}{I_1}\right)_\omega = I_\omega^* \tag{25}$$

The Fig. 12 shows a normalised third harmonic in blue for the control scheme as in Eq. 17. Only at higher frequencies near the bandwidth, the open-loop follows the amplitude threshold . At lower and middle frequencies the open-loop plot is well above the threshold. Therefore, multiple resets can occur if any reference in this region is followed.

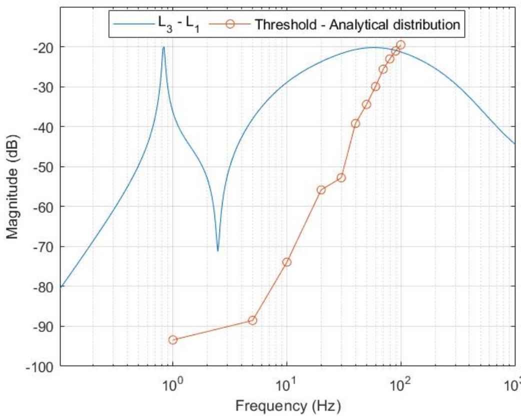

Fig. 12: Mapping of ideal closed loop sensitivity to open loop

G. Steps to find the non multiple reset criteria

To find the amplitude threshold of higher-order harmonics to avoid excessive resets, the step-wise procedure is given below.

1) In the Eq. 19, set $A_1 = 1\,(0)$ dB and choose any θ_1
2) Set m as $2e03$ to consider first $1e03$ odd harmonics
3) Calculate the higher harmonics phase by Eq. 20
4) Select a range of frequencies in log-space. Choose a frequency ω in this range and time t.
5) Distribute the amplitude $(A_n)_\omega$ of higher harmonics by analytical distribution using the closed loop sensitivity as shown in Eq. 22. Set $k_{gain} = 0$ (dB) and increment n till $n = m$
6) Compute the Eq. 19 for respective higher harmonic phases and amplitudes and plot the result
7) Check for multiple zero crossings. If no, then move to next step. If yes, then lower the k_{gain} and repeat step 6. Continue until a k_{gain} is found which results in no multiple zero crossings
8) Repeat step 4 to step 7 for various frequencies ω to obtain a ideal normalised input to reset element plot as shown in Fig. 11 and 14c
9) Map the ideal normalised sensitivity to open loop by Eq. 24 as to result in Fig. 12 and 14d

IV. ILLUSTRATIVE EXAMPLE

To validate the theory in the previous section an illustrative example is presented in this section. The plant in this example is a precision motion stage with three degrees of freedom. An image of the plant is shown in Fig. 13. The main stage in the center is guided by leaf flexures. The plant is actuated by three Lorentz actuator and consists of a 10 nm resolution laser encoder. The laser encoder measures the position of the mass being actuated. For simplicity, only one Lorentz actuator (marked by 1) is used for actuation. The system is collocated. A fit on the identified plant transfer function is represented by Eq. 26. The plant has a resonance peak of around 14 Hz. The higher harmonics will have resonance around 4.67 Hz and below.

$$P(s) = \frac{9836}{s^2 + 8.373\,s + 7376} \tag{26}$$

A new structure of controller developed recently by N. Karbasizadeh is shown in Eq. 27. The controller is designed for a bandwidth ω_c of 150 Hz. The controller provides 20° of phase lead at bandwidth as shown in the Fig. 14a.The reset part, that is H_n together with lead L_{FORE} provides 10° The linear part provides 10° of phase.The parameters for the shown are given in table I.

$$C_1 = \left(\frac{s/\omega_y + 1}{s/\omega_f + 1}\right)$$

$$H_n = \frac{1}{s/\omega_{r\alpha} + 1}\ \gamma$$

$$C_2 = k_p\left(\frac{L_{FORE}}{C_1}\right)\left(1 + \frac{\omega_i}{s}\right)\left(\frac{s/\omega_d + 1}{s/\omega_t + 1}\right)\left(\frac{1}{s + w_f}\right)^2 \tag{27}$$

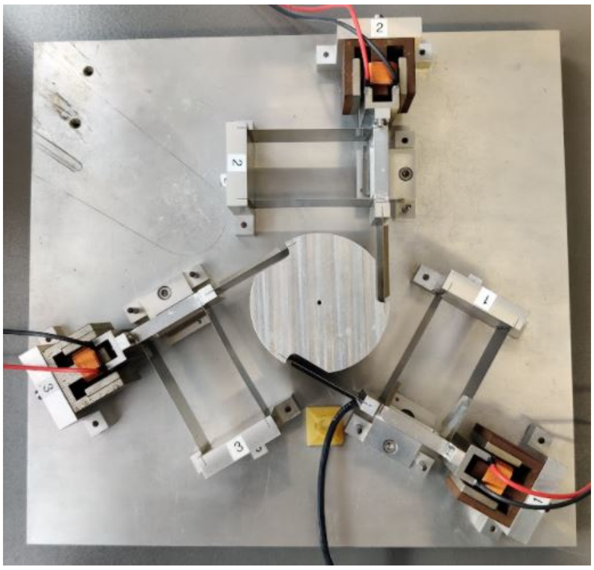

Fig. 13: Plant - 3DOF precision motion stage

where,

$$L_{FORE} = \left(\frac{s/\omega_r + 1}{s/\omega_f + 1}\right) \tag{28}$$

ω_c	ω_y	ω_r	α	γ	ω_i	ω_d	ω_t	ω_f
150 Hz	$\omega_c/3$	$1.2\,\omega_c$	0.85	0.1	$\omega_c/10$	$\omega_c/1.64$	$1.64\,\omega_c$	$10\,\omega_c$

TABLE I: Parameters for the control scheme as shown in Eq. 27

In the Fig. 14a and 14b we can see a significant difference between the first harmonic and higher harmonics magnitude. This magnitude difference is due to the shifting of the corner frequency of the reset element around the bandwidth region. The Fig. 14c shows the ideal normalised sensitivity (I^*_ω). In the analytical distribution plot there is a reduction in slope around 30 Hz due to the peak of the fifth harmonic as seen in Fig. 14b.

In the Fig. 14d, the normalised open loop meets the amplitude threshold. There is change in slope in the red plot around the 30 Hz due to peak of fifth harmonic as seen in Fig. 14b. In this example, according to the section III-C to III-F, no multiple zero crossings should occur for any reference frequency. To validate the theory, a time-domain simulation is performed as seen in Fig. 15. In all these simulations a time step size of $1e-05$ was used. The number of odd harmonics considered are $1e04$ to be on a conservative side. In the Fig. 15b and 15d, the system is excited for the resonance frequency of the third and first harmonic respectively. As the threshold criteria shown in Fig. 14d is fulfilled, we can see no multiple zero crossings occurring. The Fig. 15f shows a reference of 30 Hz where multiple resets do not occur, where the normalised open-loop is above the threshold value. There can exist certain frequencies, which have normalised open-loop above the threshold but still result in no multiple zero crossings. For higher frequencies closer to bandwidth no multiple resets occur as shown in the Fig. 15g and 15h.

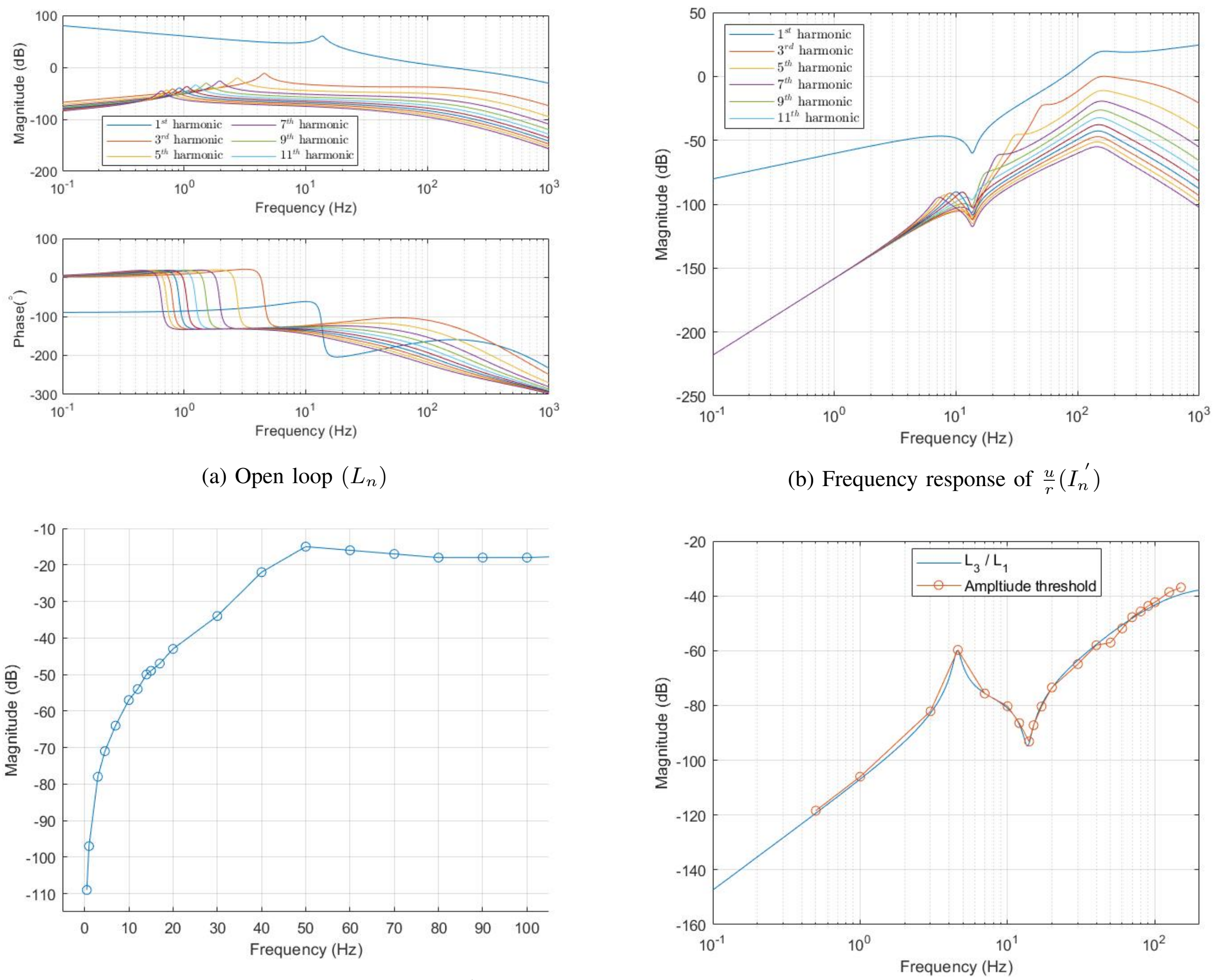

(a) Open loop (L_n)

(b) Frequency response of $\frac{u}{r}(I_n^{'})$

(c) Ideal normalised input closed-loop function (I_{ω}^{*}) to the reset element

(d) Mapping of ideal normalised input to open loop

Fig. 14: Frequency response of the control scheme shown in equation 27

V. Conclusion

This paper proposes an amplitude threshold criterion to avoid excessive zero crossings in a signal consisting of a sum of multiple sinusoids. The application of such criterion is evident in the field of reset control. The closed-loop performance of reset elements depends on the number and instant of resets. Reset control being nonlinear, closed-loop performance cannot be accurately predicted using the open-loop. Estimating the closed-loop performance analytically becomes difficult if multiple resets occur. Using numerical methods to calculate closed-loop functions is computationally expensive. To calculate the amplitude threshold, open-loop HOSIDF functions are used, which reduces computation cost. To find the threshold, first, the number of odd harmonics to consider is determined. Second, a phase for multiple resets is calculated. Third, the amplitude is distributed for higher-order harmonics. Then, the ideal input to the reset element is computed. Last, a mapping to open-loop is performed.

To validate the theory, an example of a reset control scheme that meets the amplitude threshold criterion is presented. Through the time-domain simulation, the avoidance of excessive zero crossings was confirmed. There are some aspects of this work for future research. The process of calculating the amplitude threshold has a manual part of an inspection of the number of zero crossings. An algorithm that detects zero crossings can be implemented to make the prices quicker. The number of harmonics considered for a certain frequency or range of frequencies can be optimised. Testing this theory on other reset control architecture and practical implementation can be a part of future work.

References

[1] R. M. Schmidt, G. Schitter, and A. Rankers, *The Design of High Performance Mechatronics-: High-Tech Functionality by Multidisciplinary System Integration*. Ios Press, 2020.

[2] J. Clegg, "A nonlinear integrator for servomechanisms," *Transactions of the American Institute of Electrical Engineers, Part II: Applications and Industry*, vol. 77, no. 1, pp. 41–42, 1958.

[3] I. Horowitz and P. Rosenbaum, "Non-linear design for cost of feedback reduction in systems with large parameter uncertainty," *International Journal of Control*, vol. 21, no. 6, pp. 977–1001, 1975.

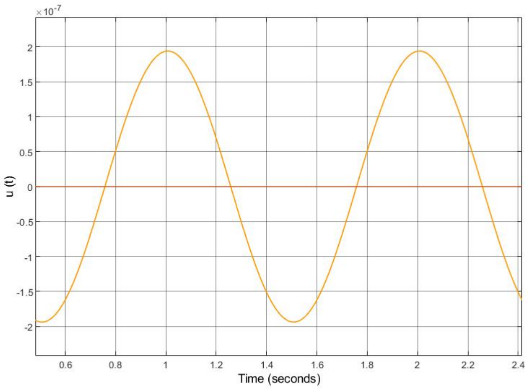

(a) $r(t) = A_0\ \sin(2\pi 1\, t)$

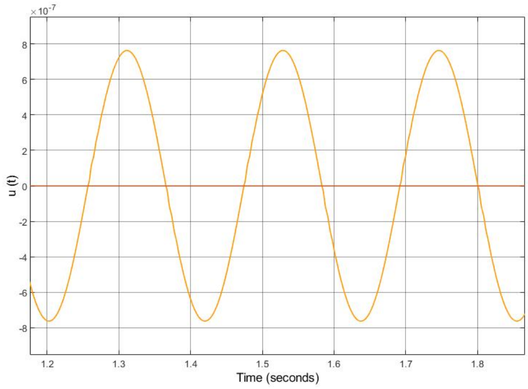

(b) $r(t) = A_0\ \sin(2\pi 4.6\, t)$

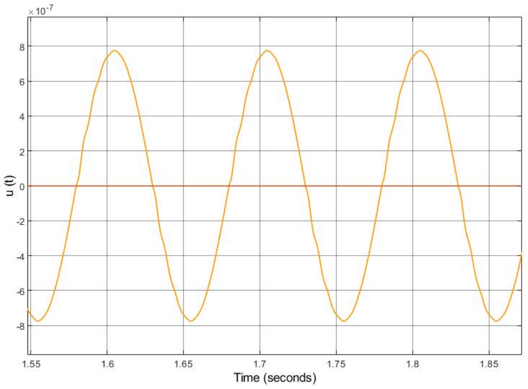

(c) $r(t) = A_0\ \sin(2\pi 10\, t)$

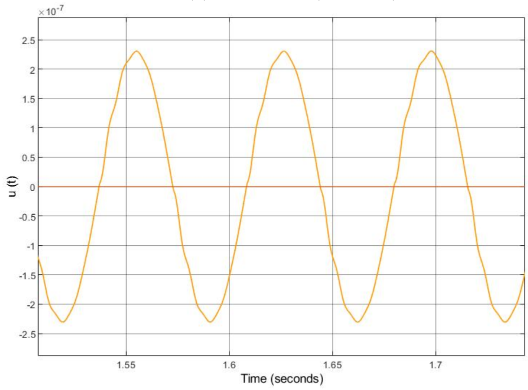

(d) $r(t) = A_0\ \sin(2\pi 14\, t)$

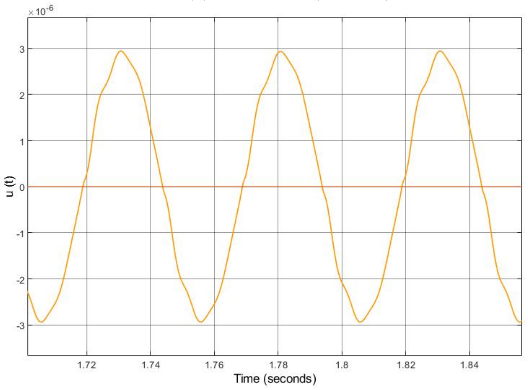

(e) $r(t) = A_0\ \sin(2\pi 20\, t)$

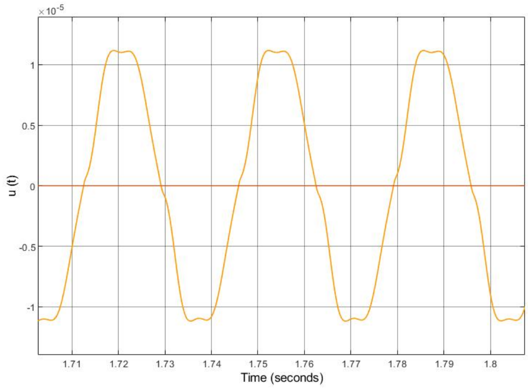

(f) $r(t) = \sin(2\pi 30\, t)$

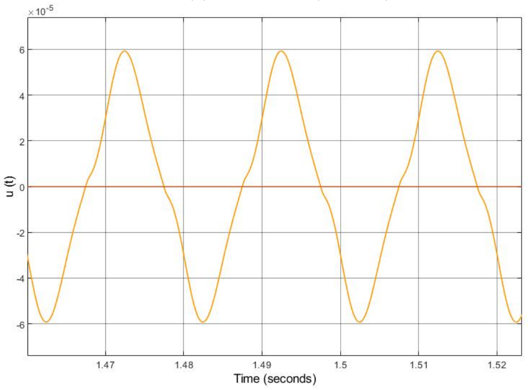

(g) $r(t) = A_0\ \sin(2\pi 50\, t)$

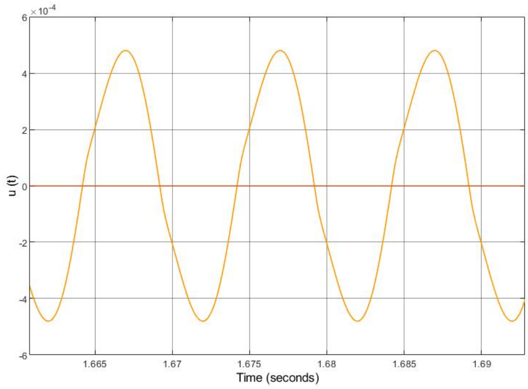

(h) $r(t) = A_0\ \sin(2\pi 100\, t)$

Fig. 15: Time response of the control scheme shown in Eq. 27 with $A_0 = 0.2mm$

[4] L. Hazeleger, M. Heertjes, and H. Nijmeijer, "Second-order reset elements for stage control design," in *2016 American Control Conference (ACC)*. IEEE, 2016, pp. 2643–2648.
[5] N. Saikumar, R. K. Sinha, and S. H. HosseinNia, ""constant in gain lead in phase" element–application in precision motion control," *IEEE/ASME Transactions on Mechatronics*, vol. 24, no. 3, pp. 1176–1185, 2019.
[6] N. Karbasizadeh, N. Saikumar, and S. H. HosseinNia, "Fractional-order single state reset element," *arXiv preprint arXiv:2009.11131*, 2020.
[7] A. Vidal and A. Baños, "Reset compensation for temperature control: Experimental application on heat exchangers," *Chemical Engineering Journal*, vol. 159, no. 1-3, pp. 170–181, 2010.
[8] V. Ghaffari, P. Karimaghaee, and A. Khayatian, "Reset law design based on robust model predictive strategy for uncertain systems," *Journal of Process Control*, vol. 24, no. 1, pp. 261–268, 2014.
[9] E. Akyüz, N. Saikumar, and S. H. HosseinNia, "Reset control for vibration disturbance rejection," *IFAC-PapersOnLine*, vol. 52, no. 15, pp. 525–530, 2019.
[10] Y. Guo, L. Xie, and Y. Wang, *Analysis and design of reset control systems*. Institution of Engineering and Technology, 2015.
[11] A. Vidal and A. Banos, "Qft-based design of pi+ ci reset compensators: application in process control," in *2008 16th Mediterranean Conference on Control and Automation*. IEEE, 2008, pp. 806–811.
[12] O. Beker, C. Hollot, Y. Chait, and H. Han, "Fundamental properties of reset control systems," *Automatica*, vol. 40, no. 6, pp. 905–915, 2004.
[13] Y. Li, G. Guo, and Y. Wang, "Nonlinear mid-frequency disturbance compensation in hard disk drives," *IFAC Proceedings Volumes*, vol. 38, no. 1, pp. 31–36, 2005.
[14] Y. Guo, Y. Wang, and L. Xie, "Frequency-domain properties of reset systems with application in hard-disk-drive systems," *IEEE Transactions on Control Systems Technology*, vol. 17, no. 6, pp. 1446–1453, 2009.
[15] P. Nuij, O. Bosgra, and M. Steinbuch, "Higher-order sinusoidal input describing functions for the analysis of non-linear systems with harmonic responses," *Mechanical Systems and Signal Processing*, vol. 20, no. 8, pp. 1883–1904, 2006.
[16] K. Heinen, "Frequency analysis of reset systems containing a clegg integrator: An introduction to higher order sinusoidal input describing functions," 2018.
[17] A. A. Dastjerdi, A. Astolfi, N. Saikumar, N. Karbasizadeh, D. Valerio, and S. H. HosseinNia, "Closed-loop frequency analysis of reset control systems," *arXiv preprint arXiv:2001.10487*, 2020.
[18] N. Saikumar, K. Heinen, and S. H. HosseinNia, "Loop-shaping for reset control systems–a higher-order sinusoidal-input describing functions approach," *arXiv preprint arXiv:2008.10908*, 2020.
[19] C. Cai, A. A. Dastjerdi, N. Saikumar, and S. H. HosseinNia, "The optimal sequence for reset controllers," *arXiv preprint arXiv:2005.13877*, 2020.
[20] N. Blachman, "Zero-crossing rate for the sum of two sinusoids or a signal plus noise (corresp.)," *IEEE Transactions on Information Theory*, vol. 21, no. 6, pp. 671–675, 1975.

5 Conclusion

5.1 Research objective and results

The objective of this thesis is to find a amplitude threshold criterion on the of higher-order harmonics such that no multiple resets occur. The number and instant of resets occurring are vital in approximating the closed-loop sensitivities. In [9], Saikumar et al. proposed an open-loop HOSIDF based approximation for calculating the closed-loop sensitivities for a control scheme with a reset element. This approximation assumes that no excessive resets (zero crossings) are caused by higher harmonics. However, the paper did not propose any criteria for such an assumption. This report provides an amplitude threshold criteria on higher-order harmonics to avoid the multiple zero crossings.

The procedure to calculate the amplitude threshold on higher-order harmonics is discussed in section III.G (chapter 4). The reset signal being a multi-sine signal, parameters needed to compute the threshold are phase, amplitude and number of higher-order harmonics. First, the number of odd harmonics to consider is determined depending on the reference and bandwidth. Second, a phase for each odd higher-order harmonics is calculated which is optimum for multiple resets. Third, the amplitude of higher-order harmonic is distributed by computing the closed-loop response (sensitivity) of the reset signal to the reference. These amplitudes of higher-order harmonics are normalised by the third harmonic. Next, the first and higher-order sinusoids are summed and inspected for multiple zero crossings. Last, a mapping from the closed-loop to the open-loop is performed. Such a mapping assists to determine the denial of multiple resets from the open-loop response of a reset control system. The chapter 4 provides two examples. The examples consist of a control scheme with linear filters, reset element and second-order plant. In the first example, the amplitude threshold is not satisfied by the system and multiple zero crossings occur. To validate the theory, in the second example a reset controller is tuned to satisfy the amplitude threshold. Through the time-domain simulation, the denial of multiple resets is confirmed.

5.2 Recommendations

- The steps to calculate the amplitude threshold contains a manual part. After plotting the summation of the first and higher-order harmonics, we need to manually check for multiple zero crossings. This part can be automated by implementing an algorithm that outputs the number of zero crossings in a multi-sine signal.
- The amplitude threshold theory is to be tested on reset elements with multiple reset states.
- The amplitude threshold theory is to be tested on control architecture on multiple reset elements. Before calculating the threshold, first, the closed-loop approximation of a multi-reset element control scheme using HOSDIF should be computed.
- The effect of noise and disturbance on amplitude threshold needs investigation. A study on how to calculate amplitude threshold for a system with multiple inputs can be looked into.
- A general amplitude distribution that is valid for a certain control scheme can ease the process of finding the threshold and save some computing power. Along with this, the mapping function can be further investigated.
- Effect of the parameters like cutoff frequency of reset elements, number of higher-order harmonics to be considered and reset value γ on amplitude threshold is to be studied.
- Providing tuning guidelines for a controller that satisfies the amplitude threshold is important for future work.
- Implementation of a control scheme that follows the threshold on practical setup is the next step.

Appendix A Amplitude distribution 2

In the Eq. 15 (chapter 4), the amplitude A_n can also be distributed by -2 slope behaviour in Bode plot. The higher harmonics have a second-order attenuation. To mimic such a behaviour, harmonics are distributed as shown in Fig. 3. This distribution is similar to second-order LPF magnitude behaviour and is represented by Eq. 1, where the cutoff frequency is the bandwidth of the controller. Here, all the odd harmonics (≥ 3) of a reference will have the same amplitude until the n^{th} harmonic frequency is higher than the bandwidth. In the Fig. 5 (chapter 4), we see that for a frequency, as the harmonic count increases, the magnitude decreases. Also, each ascending harmonic has descending gain. Thus, the -2 slope distribution can be conservative. The -2 slope distribution is a generalised method and is valid for any reset systems which attenuates with -2 slope. While the analytical distribution will change as the reset element is changed. An illustrative example of finding the amplitude threshold using this amplitude distribution is shown in appendix B.

$$A_n(n\omega) = \left| \frac{k_{gain}}{((s/\omega_a)^2 + 2s\beta/w_a + 1)} \right| \tag{1}$$

where, $n \in odd\, N \geq 3$

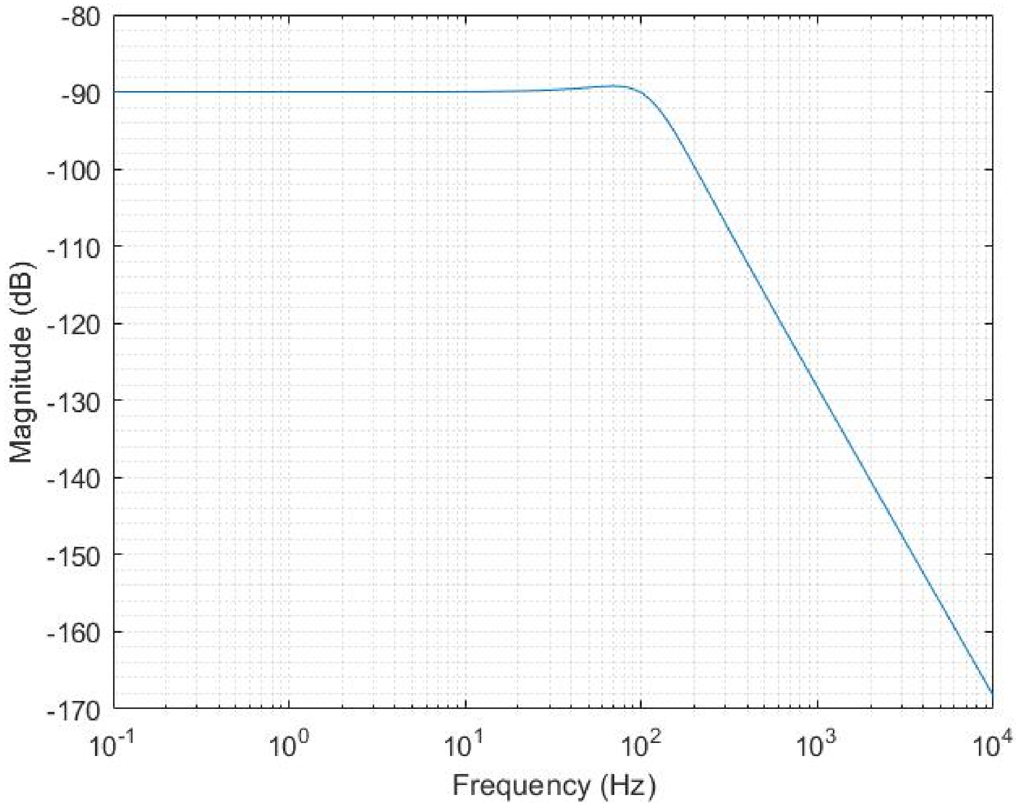

Figure 3: -2 slope amplitude distribution

Appendix B Non multiple reset threshold analysis for error signal

As the amplitude threshold criteria is valid for sinusoidal signals in general, an example for the error signal of the architecture shown in Eq. 23 (chapter 4) is illustrated in this section. The error signal is not used as the reset signal hence this example is only for demonstration. The error signal is input to filter C_1, this will alter the Eq. 19 (chapter 4) and 20 (chapter 4) to 2 as shown below. The plant is described by the Eq. 3 In the Fig. 4, the normalised open loop is under the threshold for all the frequencies. Hence, no multiple resets should occur for any reference frequency. From the Fig. 4c, 4d, 4e and 4f, it is confirmed that no multiple results occur.

$$\begin{aligned} &I_n^{'} = \frac{e}{r} = S_n \\ &\frac{L_3}{L_1} = \frac{I_3}{I_1} \frac{-C_1}{Sl_{bl}(3\omega)L_1(1+L_1)|C_1 S_1|\angle(n(C_1 S_1))} \end{aligned} \tag{2}$$

$$P(s) = \frac{3.038\,e04}{s^2 + 0.7413\,s + 243.3} \tag{3}$$

ω_c	ω_y	ω_r	α	γ	ω_i	ω_d	ω_t	ω_f
100 Hz	$\omega_c/3$	$1.2\,\omega_c$	1.07	0	$\omega_c/10$	$\omega_c/1.5$	$1.5\,\omega_c$	$10\,\omega_c$

Table 1: Parameters for the control scheme as shown in equation 23, chapter 4

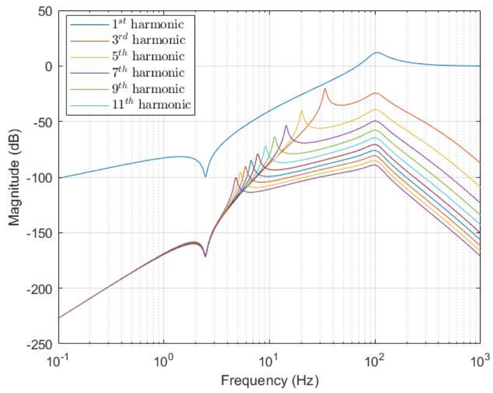

(a) Frequency response of $\frac{e}{r}(S_n)$

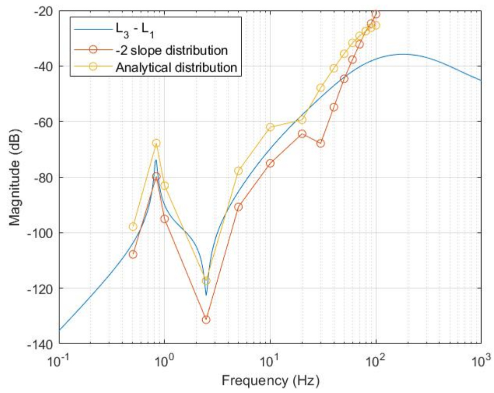

(b) Mapping of ideal closed loop signal to open loop

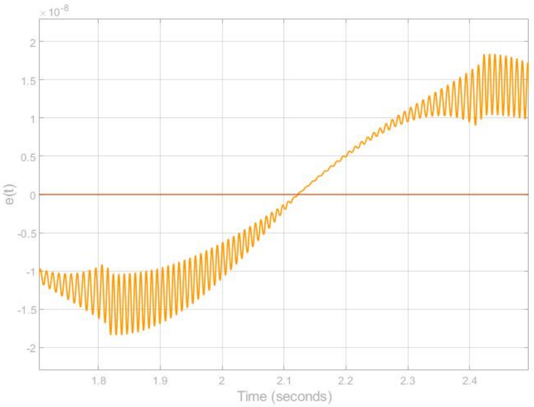

(c) $r(t) = A_0 \sin(2\pi 0.83\, t)$

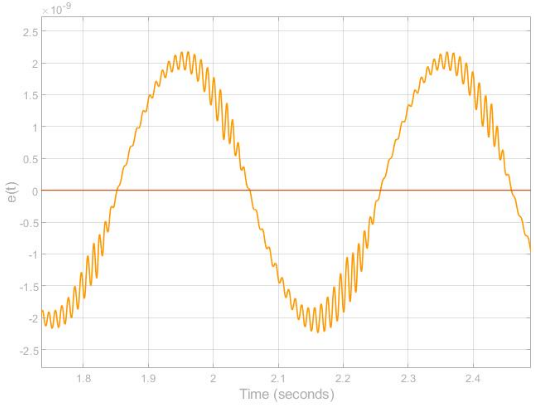

(d) $r(t) = A_0 \sin(2\pi 2.47\, t)$

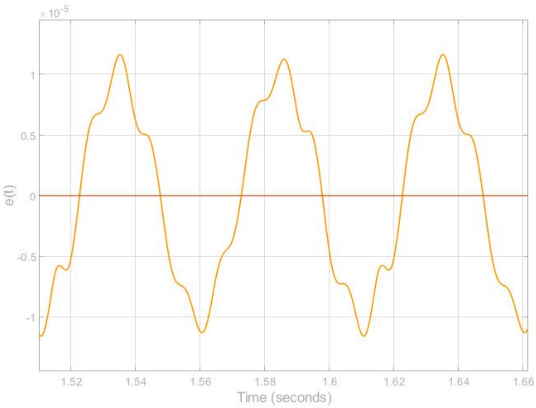

(e) $r(t) = A_0 \sin(2\pi 20\, t)$

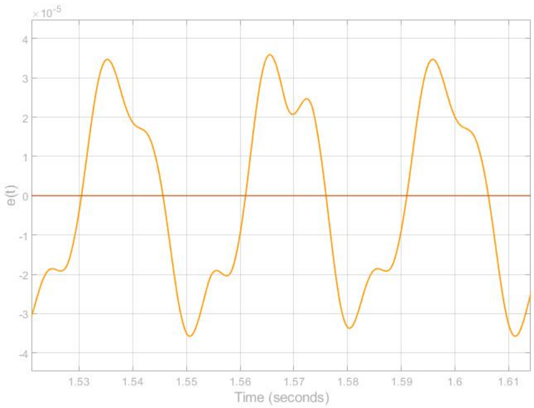

(f) $r(t) = A_0 \sin(2\pi 30\, t)$

Figure 4: Frequency and time response of the control scheme shown in Eq. 27 (chapter 4) with $A_0 = 0.2$ mm

Appendix C Effect of cutoff frequency ω_r (FORE) on the amplitude threshold

This section presents a comparison of three controllers on the amplitude threshold for higher-order harmonics. When calculating the amplitude threshold, it is important to know whether to calculate the threshold every time we change the parameters of the reset element. We know that for each ω_r, the higher order harmonics change. But is this change significant enough to make a difference in amplitude threshold? This section sheds light on that question.

The controller follows the architecture shown in Eq. 23 (chapter 4). The controllers (FORE) have three different cutoff frequencies ω_r and the rest of the parameters being the same. The cutoff frequency being $1.2\omega_c$, $0.5\omega_c$ and $0.1\omega_c$. The rest of the parameters can be found in table I (chapter 4). The Fig. 5a shows how the higher-order vary with respect to third harmonic for different ω_r. The difference is low, especially for cutoff frequencies away from bandwidth. Fig. 5c shows how amplitude threshold varies to change in cutoff frequency of FORE. Again there is no significant difference. At the peak of the third and fifth harmonic (u/r) the lower cutoff frequency has a lower threshold due to high peaks of higher harmonics. To conclude, calculating the threshold for cutoff frequency around bandwidth and using the same for tuning the controller is a good approximation.

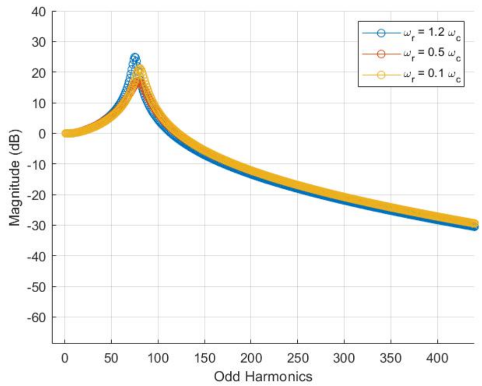

(a) Amplitude distribution of higher harmonics normalised by third harmonic

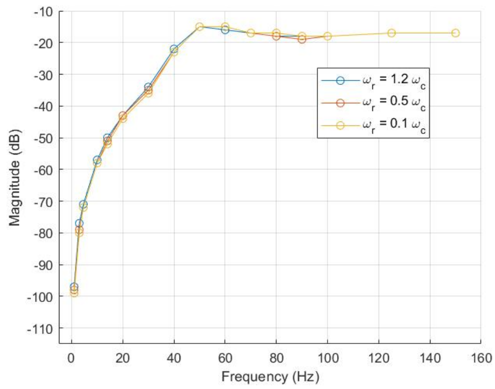

(b) Ideal input to reset element normalised by first harmonic

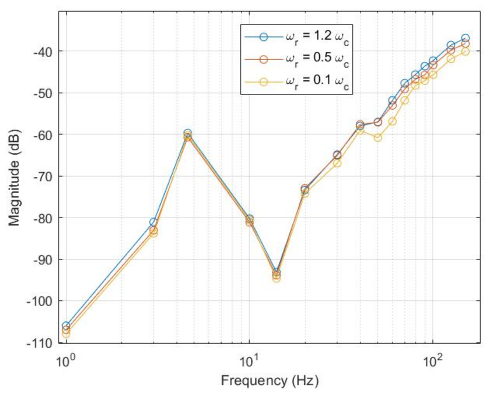

(c) Amplitude threshold for higher order harmonics mapped to normalised open loop (L_3/L_1)

Figure 5: Effect of FORE cutoff frequency ω_r on higher order harmonics and amplitude threshold for them

Appendix D Effect of number of harmonics on the amplitude threshold

An important question for calculating the amplitude threshold is to determine the number of odd harmonics to be taken into account. The number of odd harmonics has a direct effect on the amplitude threshold value and computation time. The ideal scenario is to obtain a threshold close enough to one calculated by considering more harmonics and then putting some tolerance limit on it. Considering a higher number of harmonics seems a good choice but it also depends on the sampling frequency. As an optimum phase is associated with every harmonic, aliasing can cause a mismatch of phase and frequency and eventually change the amplitude threshold.

The table 2 presents the variation in amplitude threshold to the number of odd harmonics for some frequencies. The amplitude threshold in the table is calculated for the control scheme shown in Eq. 23 and table I (chapter 4). Here the bandwidth of the controller is 150 Hz. For frequencies that are around two orders less than the bandwidth, more numbers need to be considered. In the table 2, for 1 Hz, considering 50 and 100 odd harmonics provide a higher threshold, which can lead to multiple zero crossings. For frequencies that are around one order lower than the bandwidth, the threshold does not deviate much for 50 to 10000 odd harmonics. To conclude, when calculating amplitude threshold, for lower frequencies considering $1000 - 5000$ odd harmonics and for higher frequencies $100 - 1000$ odd harmonics are good conservative approximation.

Frequency (Hz)	Amplitude threshold (dB)					
	Number of odd harmonics					
	50	100	500	1000	5000	10000
1	-81.0	-99.0	-106.0	-106.0	-106.0	-106.0
4.6	-56.7	-58.7	-59.7	-59.7	-59.7	-59.7
10	-79.2	-80.3	-80.3	-80.3	-80.3	-80.3
14	-93.1	-93.1	-93.1	-93.1	-93.1	-93.1
20	-73.4	-73.4	-73.4	-73.4	-73.4	-73.4
30	-64.9	-64.9	-64.9	-64.9	-64.9	-64.9
40	-58.0	-58.0	-58.0	-58.0	-58.0	-58.0
50	-57.0	-57.0	-57.0	-57.0	-57.0	-57.0

Table 2: Effect of number of harmonics on the amplitude threshold

Appendix E Plant identification

To determine the transfer function for the Spyder motion stage, system identification was performed. Fig. 13 (chapter 4) shows the picture of the motion stage. A chirp signal ranging from 1 Hz to 1000 Hz was applied to the motion stage with 1.01% increase in the frequency. The period of each frequency was 300 ms with a sampling frequency of 10 KHz. The Fig. 6 shows the identified Bode plot and coherence plot. For the range, 1 Hz to 1000 Hz the coherence value is one, which is ideal. The plant has 4 masses, but the centre mass is dominant. The system is collocated as the mass 1 is actuated and measured. Mass 2 and 3 are considered parasitic motion components. Hence it is expected to have two poles close to each other as mass 1 is relatively high. The same is found in the identification plot, with poles between 12 Hz and 14 Hz. The Fig. 7 shows a second-order fit to identification. The transfer function of the fit is represented by Eq.22 (chapter 4). The MATLAB code for this section can be found in the last appendix of this report.

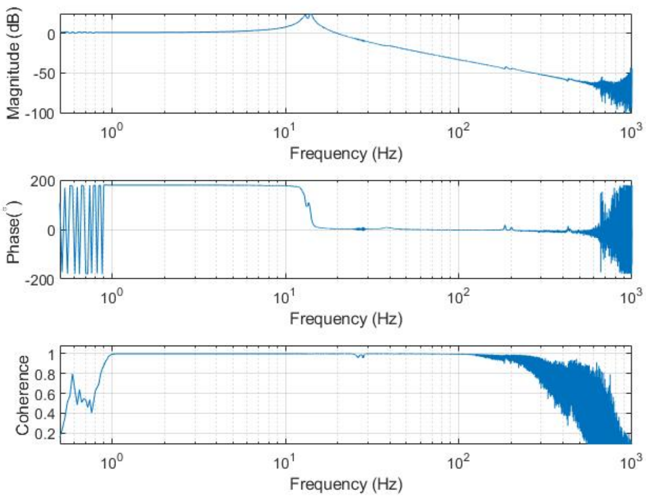

Figure 6: Bode plot of the plant (motion stage) for a chirp signal along with the coherence plot

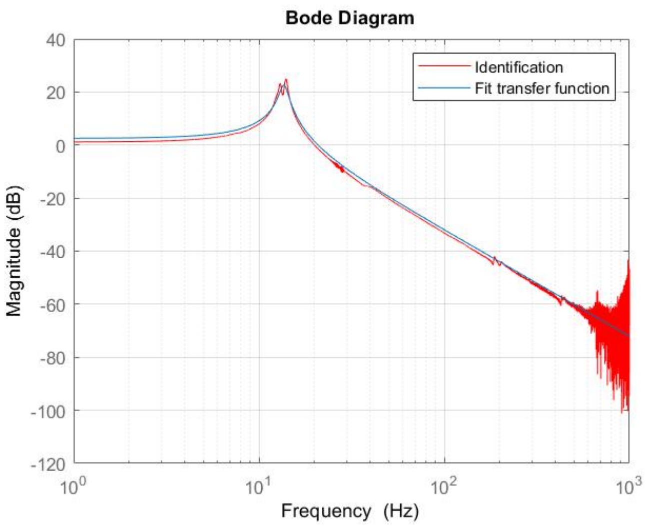

Figure 7: A transfer function fit to the identified Bode plot of the plant

Appendix F Stability analysis of reset systems

This section checks for the H_β condition for the stability of the reset closed-loop system represented by Eq. 23 (chapter 4). The corresponding closed-loop state A matrix (A_{cl}) and matrix P from Eq. 2 (chapter 4) are shown below. All the eigenvalues of P are positive, which indicates positive definite P. The values of β and P_ρ found are $4.9388e-10$ and $2.0320e-08$ respectively. All of the above information confirms the stability of the closed-loop reset system. To solve the matrix inequality, the YALMIP solver was used. The download link and installation instructions of the solver are provided in the MATLAB code, found in the last appendix of this report.

$$A_{cl} = \begin{pmatrix} -0.73 & -0.36 & -0.17 & -0.082 & -0.073 & -0.04 & -0.032 & -0.017 & -7.3e-3 & -3.4e-3 \\ 0.59 & 0 & 0 & 0 & 0 & 0 & 0 & 0 & 0 & 0 \\ 0 & 0.29 & 0 & 0 & 0 & 0 & 0 & 0 & 0 & 0 \\ 0 & 0 & 0.15 & 0 & 0 & 0 & 0 & 0 & 0 & 0 \\ 0 & 0 & 0 & 0.037 & 0 & 0 & 0 & 0 & 0 & 0 \\ 0 & 0 & 0 & 0 & 0.037 & 0 & 0 & 0 & 0 & 0 \\ 0 & 0 & 0 & 0 & 0 & 0.018 & 0 & 0 & 0 & 0 \\ 0 & 0 & 0 & 0 & 0 & 0 & 0.018 & 0 & 0 & 0 \\ 0 & 0 & 0 & 0 & 0 & 0 & 0 & 9.2e-3 & 0 & 0 \\ 0 & 0 & 0 & 0 & 0 & 0 & 0 & 0 & 2.3e-3 & 0 \end{pmatrix}$$

$$P = \begin{pmatrix} 6.4e-6 & 1.1e-6 & 1.1e-6 & 2.8e-7 & 4.4e-7 & 1.4e-7 & 1.9e-7 & 6.3e-8 & 5.8e-8 & -4.3e-14 \\ 1.1e-6 & 2.9e-6 & 6.2e-7 & 7.5e-7 & 3.5e-7 & 3.7e-7 & 1.6e-7 & 1.5e-7 & 5.3e-8 & 4.6e-9 \\ 1.1e-6 & 6.2e-7 & 9.4e-7 & 2.6e-7 & 5.0e-7 & 1.5e-7 & 2.3e-7 & 6.9e-8 & 7.2e-8 & 5.9e-13 \\ 2.8e-7 & 7.5e-7 & 2.6e-7 & 4.8e-7 & 2.2e-7 & 2.7e-7 & 1.1e-7 & 1.1e-7 & 4.1e-8 & 6.9e-13 \\ 4.4e-7 & 3.5e-7 & 5.0e-7 & 2.2e-7 & 7.9e-7 & 1.8e-7 & 4.1e-7 & 9.7e-8 & 1.4e-7 & -1.3e-13 \\ 1.4e-7 & 3.7e-7 & 1.5e-7 & 2.7e-7 & 1.8e-7 & 3.3e-7 & 9.7e-8 & 1.8e-7 & 5.1e-8 & -9.3e-14 \\ 1.9e-7 & 1.6e-7 & 2.3e-7 & 1.1e-7 & 4.1e-7 & 9.7e-8 & 3.0e-7 & 5.3e-8 & 1.5e-7 & 6.4e-13 \\ 6.3e-8 & 1.5e-7 & 6.9e-8 & 1.1e-7 & 9.7e-8 & 1.8e-7 & 5.3e-8 & 1.3e-7 & 2.9e-8 & 6.9e-13 \\ 5.8e-8 & 5.3e-8 & 7.2e-8 & 4.1e-8 & 1.4e-7 & 5.1e-8 & 1.5e-7 & 2.9e-8 & 1.3e-7 & -1.8e-13 \\ -4.3e-14 & 4.6e-9 & 5.9e-13 & 6.9e-13 & -1.3e-13 & -9.3e-14 & 6.4e-13 & 6.9e-13 & -1.8e-13 & 2.0e-8 \end{pmatrix}$$

$$eigen(P) = \begin{pmatrix} 1.4e-8 \\ 1.7e-8 \\ 2.0e-8 \\ 1.2e-7 \\ 1.5e-7 \\ 3.7e-7 \\ 4.5e-7 \\ 1.2e-6 \\ 3.0e-6 \\ 7.1e-6 \end{pmatrix}$$

Appendix G MATLAB codes

To calculate amplitude threshold:
`https://drive.google.com/file/d/1_V1ndqsqnokQYpqQnaG5pPwtqYYP9V2P/view?usp=sharing`

Simulink file:
`https://drive.google.com/file/d/1Fck06-WXlQnSf0xVvWaS0D5tUf7oiEWy/view?usp=sharing`

Plant identification:
`https://drive.google.com/file/d/1mlgJiUsw0pGYWqMpDLNsT-wdWf1d4zlB/view?usp=sharing`

Stability analysis:
`https://drive.google.com/file/d/1py4sG5ZTUtIQZdXz9pzhu3fX18GB4r0L/view?usp=sharing`

References

[1] URL: `https://www.asml.com/news/stories/2020/asml-wins-semi-americas-award-for-euv`.

[2] URL: `https://www.pcasilicon.com/wp-content/uploads/sites/4008/2017/02/20_02_2.jpg`.

[3] URL: `https://www.shutterstock.com/image-photo/silicon-wafer-die-attach-machine-semiconductor-1015265728`.

[4] JC Clegg. “A nonlinear integrator for servomechanisms”. In: *Transactions of the American Institute of Electrical Engineers, Part II: Applications and Industry* 77.1 (1958), pp. 41–42.

[5] Leroy Hazeleger, Marcel Heertjes, and Henk Nijmeijer. “Second-order reset elements for stage control design”. In: *2016 American Control Conference (ACC)*. IEEE. 2016, pp. 2643–2648.

[6] Isaac Horowitz and Patrick Rosenbaum. “Non-linear design for cost of feedback reduction in systems with large parameter uncertainty”. In: *International Journal of Control* 21.6 (1975), pp. 977–1001.

[7] Nima Karbasizadeh, Niranjan Saikumar, and S Hassan HosseinNia. “Fractional-Order Single State Reset Element”. In: *arXiv preprint arXiv:2009.11131* (2020).

[8] Nima Karbasizadeh et al. “Benefiting from Linear Behaviour of a Nonlinear Reset-based Element at Certain Frequencies”. In: *arXiv preprint arXiv:2004.03529* (2020).

[9] Niranjan Saikumar, Kars Heinen, and S Hassan HosseinNia. “Loop-shaping for reset control systems–A higher-order sinusoidal-input describing functions approach”. In: *arXiv preprint arXiv:2008.10908* (2020).